Yu et al. *Microsystems & Nanoengineering* (2026)12:45
https://doi.org/10.1038/s41378-025-01118-8

Microsystems & Nanoengineering
www.nature.com/micronano

REVIEW ARTICLE Open Access

Sensitivity enhancement of surface plasmon resonance biosensors based on versatile nanostructures: principle, fabrication, and illustrative applications

Xiantong Yu[1]✉, Yufeng Yuan[2]✉, Jun Zhou[1], Min Chang[1], Shuwen Zeng[3]✉ and Songlin Zhuang[1]

Abstract

Surface plasmon resonance (SPR) biosensoris a new type of high sensitivity, real-time, label-free detection technology, which plays an increasingly important role in the biomedicine field. Considering the urgent requirement of trace detection, especially for diagnosing early-stage diseases, the demand for high detection sensitivity of sensors is increasing. In recent years, various nanostructures have been proposed to design SPR biosensors. By constructing composite nanostructures, the detection sensitivity has been significantly enhanced, which has become a promising solution to expand the application of SPR biosensors. This review systematically summarized the basic principle, fabrication and illustrative application of SPR biosensors based on versatile nanostructures. Firstly, the mechanisms of various nanostructures to enhance the detection sensitivity of SPR biosensors were clarified. Then, the preparation strategies of various nanostructures were comprehensively illustrated. In addition, this review also summarized the latest applications of SPR biosensors with different structures. Finally, this review carefully highlighted the current challenges and possible development directions in future.

Introduction

To date, SPR biosensor is a highly sensitive, real-time and label-free sensing technology based on the collective oscillation effect of free electrons on the surface of noble metals[1–4]. Free electrons on the surface of noble metals (such as gold and silver) oscillate collectively under the action of light field, forming propagating surface plasmon polaritons (PSPPs)[5,6]. Under a well-matched frequency, the incident photon drives coherent oscillations of surface electrons, the SPR effect is realized, and the resonance condition is extremely sensitive to the small change of the refractive index (RI) of the surrounding medium[7–9]. Therefore, the biosensor based on this principle can realize the real-time detection of nearby biological molecules[10–13]. With the advantages, SPR biosensor technology has rapidly become a core tool in the fields of life science, medical diagnosis and environmental monitoring[14–22]. The key performance index of SPR biosensor - detection sensitivity (usually measured by the resonant wavelength or angular shift caused by the change of RI unit)—directly determines its practical application value in the detection of trace biomarkers[23–25].

Correspondence: Xiantong Yu (xtyu@usst.edu.cn) or
Yufeng Yuan (yufengyuan@dgut.edu.cn) or
Shuwen Zeng (shuwen.zeng@cnrs.fr)
[1]Key Laboratory of Optical Technology and Instrument for Medicine, Ministry of Education, College of Optical-Electrical and Computer Engineering, University of Shanghai for Science and Technology, Shanghai, China
[2]School of Electronic Engineering and Intelligentization, Dongguan University of Technology, Dongguan, China
[3]Light, Nanomaterials, Nanotechnologies (L2n), CNRS UMR 7076, University of Technology of Troyes, Troyes, France

Notation		GST	$Ge_2Sb_2Te_5$
0D	Zero-dimensional	LECT2	Leukocyte chemokine-2
1D	One-dimensional	LSPR	Local surface plasmon resonance
2D	Two-dimensional	LSP	Local surface plasmon
AA	Ascorbic acid	LOD	Limit of detection
AuNPs	Gold nanoparticles	MTAP	MXene TA Au PEG
AuNPs@Mem	Membranes functionalized AuNPs	MOF	Metal-organic frameworks
BIC	Bound States in the Continuum	NIL	Nanoimprint lithography
BP	Black phosphorus	PDA	Polydopamine
CCD	Charge coupled device	PD-L1$^+$	Programmed cell death ligand-1 positive
CD-AuNPs	Cyclodextrin-functionalized AuNPs	PSM	Plasmon scattering microscope
CEA	Carcinoembryonic antigen	PM	Plasmon metasurface
CFP-10	10 kDa culture filtrate protein	PVD	Physical vapor deposition
CNTs	Carbon nanotubes	PVP	Polyvinyl pyrrolidone
CQ	Chloroquine phosphate	PVT	Physical vapor transport
CTAB	Hexadecyltrimethylammonium bromide	Quasi-BIC	Quasi Bound States in the Continuum
CVD	Chemical vapor deposition	RF	Radio frequency
CTCs	Circulating tumor cells	RI	Refractive index
DDA	Discrete dipole approximation	RIU	Refractive index unit
DLW	Direct laser writing	SEM	Scanning electron microscope
EBL	Electron beam lithography	SNR	Signal-to-noise ratio
FDTD	Finite-difference time-domain	SPR	Surface plasmon resonance
FEM	Finite element method	SPRM	Surface plasmon microscopes
FOM	Figure of Merit	SWCNTs	Single-walled carbon nanotubes
FIB	Focused ion beam	TB	Tuberculosis
FWHM	Full width at half maximum	TBG	Twisted bilayer graphene
GHS	Goos-Hänchen shift	TDN	Triple DNA nanoswitch
		TMDs	Transition metal dichalcogenides
GHP	Grotthuss-Hankins-Prigogine	UV	Ultraviolet
GNR	Gold nanorods	VCDG	Vertically coupled double-layer gratings
GO	Graphene oxide	vdWhs	Van der Waals heterostructures

Traditional SPR biosensors mainly rely on uniform noble metal films as the sensing interface[26]. Its sensitivity is limited by the lack of electromagnetic field attenuation length (approximately 200 nm) and local field enhancement ability, which has gradually been difficult to meet the demand[27–29]. In recent years, through cross fusion of nanophotonics and materials science, SPR technology has experienced a paradigm shift from "thin film sensing" to "precise control of nanostructures"[30–32]. Through the customized design of nanostructures, enhancing local electromagnetic fields, expanding sensing areas and increasing bio-molecular binding sites have become the key directions to break through the bottleneck of existing technologies[33–36].

The first is the composite structure of metal nanoparticles and metal films, which can improve the detection sensitivity through the coupling effect of SPR and local surface plasmon resonance (LSPR)[37–39]. For example, Chen et al. designed a $MoSe_2$/ZnO composite sensing film plasmonic sensor for non-enzymatic glucose detection[40], which obtained a 72.17 nm(mg/mL) detect sensitivity, and the detection limit is 4.16 μg/mL. Wulandari et al. introduced the SPR chip modified with MoS_2-MoO_3

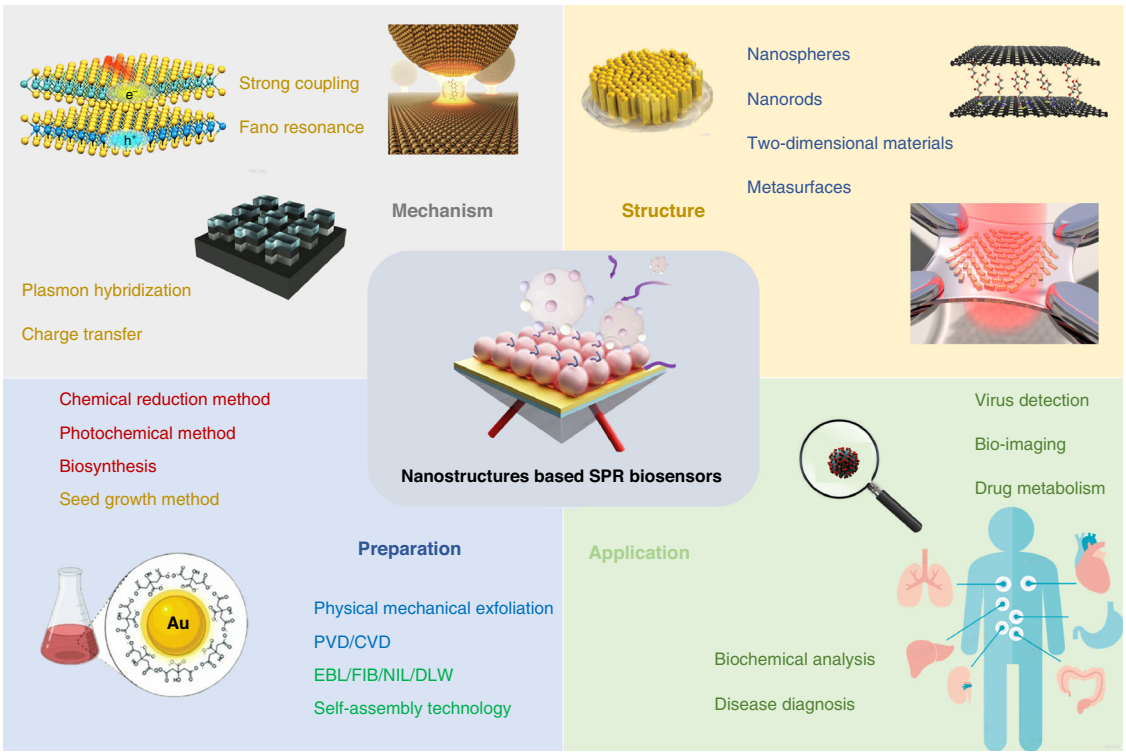

Fig. 1 Illustration of sensitivity enhancement strategies of SPR biosensors including mechanism, structure, preparation, and application

nanoflowers prepared by hydrothermal method to detect the tuberculosis (TB) marker of 10 kDa culture filtrate protein (CFP-10)[41], and obtained a response ten times higher than that of single plasmonic gold film. Liu et al. proposed a SPR strategy for functionalizing gold nanoparticles using red blood cell membranes and Circulating tumor cells (CTCs) membranes (AuNPs@Mem)[42]. It is used for high sensitivity detection of CTCs. AuNP in AuNPs@Mem as a signal amplification molecule, obtained a detection interval from 5×10^3 to 1×10^6 particles/mL, and the measurement limit was 868.11 particles/mL.

Secondly, two-dimensional (2D) materials (such as graphene and transition metal sulfide) can enhance SPR response through interface charge transfer and exciton-plasmon coupling due to their atomic thickness, high carrier mobility and tunable band gap characteristics, which has gradually attracted wide attention[43–45]. Phan et al. designed a SPR biosensor combined with 2D antimonene and applied it to the detection of microRNA[46]. The detection resolution of miR-21-5p and miR-125-5p is 21.29 fM and 27.65 fM, respectively. Banerjee et al. designed a SPR biosensor based on gold film and 2D materials gallium nitride (GaN) to detect four kinds of bacteria in drinking water[47]. The highest sensitivity of Escherichia coli is approximately 2.13×10^4 nm/RIU (refractive index unit, RIU). Kumar et al. designed a SPR biosensor combined with 2D graphene oxide (GO) for real-time and label-free detection of chloroquine phosphate (CQ) in water[48]. The limit of detection values of CQ in the final detected water and real samples (serum) were 0.21 μM and 0.34 μM, respectively.

In addition, metasurface can precisely control the wavefront, phase and polarization of light through a subwavelength structure array[49,50], providing a multidimensional signal enhancement mechanism for SPR sensors[51–53]. In recent years, metasurface has been gradually used in the design of SPR biosensors. Hu et al. developed a SPR sensor[54] of selectively adjusting the resonance mode, which can either enhance the sensitivity to a theoretical maximum of approximately ~10^5 nm/RIU. The sensor achieved an detection limit for 27.5 fM for the detection of d-biotin molecule (MW = 244 Dalton). Another work by Shokova et al. investigate the sensing performance of gold silicon dioxide-gold optical cavity with nanopore array in the dielectric layer and top metal layer used finite-difference time-domain (FDTD) method[55]. By adjusting the size of the resonator and the spacing between the holes, the quality factor can reach the order of 5–7.

In this review, the methods for improving the sensitivity of SPR biosensors, which are based on diverse nanostructures, have been summarized, focusing on the theoretical explanations of different nanostructures to enhance the detection

sensitivity and the recent progress, as shown in Fig. 1. The Review is divided into four parts: the first part describes the basic mechanism of SPR biosensors based on nanostructures; The second part summarizes the preparation methods of various nanostructures; The third part discusses the design of various nanostructured SPR biosensors and their applications in ultra-high sensitivity detection; The fourth part summarizes the current situation of this research field and prospects the future development trend.

Modulation methods of SPR biosensing technology

The SPR effect of metallic materials is closely related to the RI of the medium on the metal surface. When there is a slight change in the RI of the metal surface, the position of the SPR resonance peak will also change. If the cause of this change is a variation in the amount of biological analytes near the metal material surface, the concentration level of the biological analyte can be determined based on the change of the SPR resonance[56]. Therefore, the plasmonic biosensing detection technology developed based on this principle.

Based on different test parameters, SPR biosensing technology primarily employs four modulation methods: angle modulation[57–59], wavelength modulation[60,61], phase modulation[29,62], and spatial displacement modulation[63]. The first two methods are the most widely used, and most commercial SPR detection instruments employ these two modulation methods due to their advantages of mature technology and stable and reliable results. However, angle modulation and wavelength modulation are gradually unable to meet the increasing sensitivity requirements. The third method, with high sensitivity, is currently in the stage of gradually maturing technology. Its disadvantage is that the experimental equipment is complex and relies on the quality of the optical path, which is not conducive to application promotion. The fourth method, which adopts a different measurement strategy from the above, avoids the instability caused by light intensity distribution by accurately measuring the Goos-Hänchen shift (GHS) caused by changes in RI. Therefore, it has higher accuracy and detection sensitivity, and has gradually gained attention and developed rapidly in recent years.

First, angle modulation is employed, which utilizes the light with a fixed frequency. By altering the incident angle, the intensity of the reflected light is detected as it varies with the incident angle, revealing the incident angle corresponding to the minimum reflected light intensity, namely the SPR resonance angle. Changes in the RI or concentration on the surface of plasmonic metallic thin film can be monitored through variations in the SPR angle. SPR sensors developed according to the principle of resonance angle changes are one of the earliest research directions in SPR detection, with detection sensitivity defined as the angle-dependent rate of change in RI (dθ/dRIU). There are primarily two methods for angle modulation. Firstly, the incident angle is altered through a mechanical rotating device, and SPR reflection spectra at various angles are obtained[64], subsequently determining the SPR resonance angle, then the RI change of the target analyte can be determined. The second method involves directly incidenting the light at a certain range of incident angles, with the intensity of reflected photons being detected by a charge coupled device (CCD) to reveal the reflection spectrum[65], determining the SPR angle and further obtaining the RI change of the target analyte.

Angle modulation has developed into a highly mature technology, characterized by high stability and reliable results. In situations where detection sensitivity is not particularly high or the reaction process is relatively slow, angle modulation remains a good choice. However, for the first method, it has stable performance, is constrained by the long time required for the mechanical rotation device to change the incident angle, making it disadvantageous in fast-response detection. The second method can quickly obtain reflection spectra at different angles, offering excellent real-time performance. But because the limit of the angle range or response interval of CCD, this method has a narrow detection range and is not suitable for situations where the RI of the target analyte changes significantly. Additionally, an improved intensity modulation method based on angle modulation is also a widely used modulation type. This method tracks the change in reflected light intensity at a fixed incident angle[66], with detection sensitivity defined as the rate of change in reflected light intensity to RI change (dp/dRIU). Overall, the development of angle modulation has been relatively slow. With the rapid development of wavelength modulation and phase modulation methods, the disadvantages of angle modulation in terms of detection sensitivity are continuously magnified, gradually failing to meet the needs for detection sensitivity.

The second modulation method is wavelength modulation. In this method, a broad-spectrum light source, typically white light, is used as the probe light. With a fixed incident angle, the spectrum of the reflected light is detected and analyzed to obtain the reflectance curve as a function of wavelength. The resonant wavelength is recorded, and changes in the RI of the medium are detected through changes in the resonant wavelength. This, in turn, reveals the reaction progress of the target reactant. The detection sensitivity is defined as the rate of change of wavelength to RI (dλ/dRIU). The detection device employs a spectrometer. The advantage of a wavelength-modulated SPR biosensor is that it does not require a mechanical rotating device, offers good real-time performance, and has a wide spectral detection range. However, this method has a high dependence on

the performance of the light source. The linewidth and intensity of ordinary light sources sometimes fail to meet detection requirements, and white light lasers are expensive, making them unsuitable for widespread use.

The third method is phase modulation. When light is incident on a metal surface at an angle greater than the critical angle for total reflection, in addition to significant changes in light intensity before and after reflection, the phase of p-wave (TM wave) also undergoes a drastic change, while the phase change of s-wave (TE wave) is much smaller. Therefore, s-wave can be used as a reference light, and the change in RI or concentration can be analyzed by measuring the phase difference between p-wave and s-wave in the reflected light. The detection sensitivity is defined as the angle-to-RI change rate (dΔφ/dRIU)[62]. The biggest characteristic of phase modulation is that its sensitivity is significantly improved compared to angle modulation and wavelength modulation, which has high application value in the field of micro-detection. Phase detection technology is also very suitable for real-time detection. Compared to the previous two modulation methods, phase detection technology requires more complex optical design and higher operational precision.

The final method is spatial displacement modulation. Its core idea is not to measure traditional changes in reflected light intensity, but to precisely measure the GHS caused by changes in RI and amplified by the SPR effect. SPR itself has already converted small changes in RI into shifts in resonance angle. Near the SPR point, the rate of change of GHS with respect to angle (dGHS/dθ) is much larger than the response change of reflectivity with regarding to angle (dR/dθ)[63]. This means that the same change in RI causes a much larger change in GHS than in reflected light intensity. Therefore, by measuring displacement rather than light intensity, theoretically, higher detection sensitivity can be achieved compared to traditional intensity methods. Additionally, traditional SPR sensors measure the absolute value of light intensity. As a result, they are very sensitive to noise caused by fluctuations in light source intensity, drift in detector sensitivity, and contamination on the surface of optical components. These factors directly lead to measurement errors. GHS, on the other hand, measures the movement of the light spot position, which is a relative value. As long as the spatial mode of light source is stable, the measurement of its central position is insensitive to absolute fluctuations in light intensity. This greatly reduces the system's requirements for light source stability and electronic device noise, improving the signal-to-noise ratio (SNR) and long-term measurement stability.

Sensitivity enhancement mechanisms of SPR biosensors using plasmonic nanostructures

The versatile nanostructures can improve the performance of SPR biosensors, and it has different theoretical mechanisms respective. In this section, we will discuss the theoretical description of several structures such as metal nanoparticles, 2D materials and metasurface structure for the sensitivity enhancement of SPR biosensors.

Mechanism of metal nanoparticles-based enhancement in detection sensitivity

It is widely recognized that metal nanoparticles are capable of sustaining local surface plasmon (LSP) modes, which correspond to the plasmonic oscillations of free electrons within the particles[67,68]. Owing to the radiative nature of LSP modes, they can be directly excited by incident light[69]. Therefore, in a system composed of metal nanoparticles near the metal film surface, the electromagnetic interaction between LSP and SPP modes can be realized as long as the SPP mode excitation is controlled. The direct result of this interaction is the enhanced local electric field distribution in the gap region, which is applied to improve the detection sensitivity of SPR sensor[37].

In order to describe the optical properties of SPR when metal nanoparticles interact with metal films, there is a special type of electromagnetic normal mode, the so-called "gap mode", which exhibits strong spatial localization in the interstitial region between the particle and the substrate surface[70]. Gap mode is considered to be the source of local electric field enhancement.

In fact, the simplified electromagnetic theory can explain this phenomenon qualitatively. If the radius R of the ball is very small than the wavelength of the incident light, the delay effect of the electromagnetic field can ignore, and with dielectric function $\varepsilon_1(\omega)$, which is located in the medium with dielectric constant ε_m. Then the resonant frequency corresponding to LSP excitation can be given by $\varepsilon_1(\omega) = -\varepsilon_m (l+1)/l$, where l is an integer ($l = 1,2,\ldots$)[70]. The amplitude attenuation of the electric field outside the ball is $r^{-(l+2)}$, where r is the distance from the center of the ball[71]. The dipole mode with $l = 1$ is mainly excited. Then the metal ball is close to the metal surface $\varepsilon_2(\omega)$, in this case, dipole-dipole interaction is used. This problem can be viewed qualitatively and the LSP mode is changed. However, a comprehensive treatment of this issue ought to incorporate all multipoles of the sphere, and the detailed theoretical analysis will not be reiterated herein[71].

Indeed, various numerical analysis methods based on classical electromagnetism are used for the theoretical analysis of this system. Discrete dipole approximation (DDA)[72], finite element method(FEM)[28] and FDTD methods[73] can be used to calculate the plasmonic properties of more complex nanoparticles and nanostructures. These calculation methods produce optical response of arbitrary nanoparticle geometry, it can achieve high accuracy (depending on grid density, time step, etc.)

within the classical framework. It is the main tool to deal with complex practical problems at present[74–76].

Recently, the plasmon hybridization theory provides a clear, convenient and simple method for calculating the SPR of composite nanostructures[37,77]. Plasmon hybridization theory decomposes nanoparticles or composite structures into simpler fundamental geometries, and subsequently computes the interaction or hybridization behavior of SPR in composite particles.

Due to the different SPR modes of the nanoparticles near the surface of the metal film, the SPR-LSPR energy coupling effect will occur, resulting in a very strong electric field distribution in the middle region, which is called the plasmon hybridization mechanism. The intensity of energy coupling is relying on the distance of two surfaces, and when these nanoparticles approach the metal surface, the plasmonic energy of the nanoparticles will show a strong shift. These offsets include not only the contribution of similar images generated by the interaction between nanoparticle plasmons and their images in metals, but also the hybrid offsets generated by the dynamic interaction between plasmonic modes. While the interaction consistently induces a red shift in plasmons and a decrease in nanoparticle spacing, the hybridization effect may result in either a red shift or a blue shift, depending on the relative energy levels of the plasmons associated with the nanoparticles and the surface. The electromagnetic enhancement is caused by the surface charge associated with the plasmonic oscillation and occurs at a frequency close to the plasmon energy of the film.

In the plasmon hybridization method, when the noble metal nanoparticles and noble metal nanofilms meet the spectral matching and the spacing is small enough (nanoscale), the plasmon mode between them will be strongly coupled, resulting in a new hybrid mode, which is anti-cross in spectrum[78]. The core advantage of strong coupling lies in the generation of super strong local electromagnetic “hot spots” in the gap between particles and films, and the hybrid modes that are has an extremely sensitive to the surrounding environment changes[79]. As a result, the response of the system to the change of external RI is much larger than that of a single structure, which improves the detection sensitivity of SPR sensor. It is one of the important strategies to realize ultra-high sensitivity optical sensor at present. In addition, when the strong coupling effect is applied to the SPR biosensor system, it can not only significantly improve the detection sensitivity, but also produce two coherent SPR vibration peaks due to the SPP mode splitting, so the proportional biosensor can be constructed to further improve the detection accuracy.

Mechanism of 2D materials-enhanced SPR detection sensitivity

In recent years, research on metal-2D material composite structure SPR sensors has become the hottest research direction in this field[80–82]. Some works have shown that by integrating 2D materials on the surface of metal thin films and constructing SPR sensing layers[63,83,84], significant improvements in detection performance have been achieved, especially in the research direction of biosensors, which has gradually become the mainstream choice[85,86]. For sensors with 2D material/metal composite structure, it is generally believed that the electronic property of 2D materials, that is, the Fermi energy level (work function) of 2D materials is the key to enhance the sensitivity of SPR biosensors[27,28]. When the layered 2D material contacts with the noble metal film, the continuity of Fermi level causes the generation of charge transfer[87,88]. It is found that the charge transfer mechanism between noble metal surface and graphene can obtain a large amount of excitation energy, and the direction of charge transfer will be from graphene to Au film[27]. In addition, the 2D material can also increase the surface area volume ratio and optimize the distribution of surface active sites, which enhances the specific adsorption of the sensor to biological analytes, and will further improve the detection sensitivity, providing a new path for the development of biological detection devices with high integration and high response performance[89,90].

Because this composite structure involves microscopic phenomena such as charge transfer, so the interaction between 2D materials and a series of metal surfaces can well explain by using the first principles. Taking graphene as an example[43,91], it was found that the adsorption of graphene on Al, Cu, Ag, Au and Pt (111) surfaces resulted in physical adsorption, which retained the typical electronic structure of graphene, including cone point. In the case of physical adsorption, there are short-range graphene metal interactions. These results in the shift of the Fermi level of graphene relative to the conical point, and the work function of the graphene-metal system changes significantly compared with the metal surface.

To characterize the physical adsorption and charge transfer mechanism between graphene layers and plasmonic metal, the DFT approach is employed. This model then takes only the work functions of isolated graphene and metal as input parameters, and predicts the work function shift of the metal–graphene system.

The work function W of grapheme-metal system is given by the Fermi energy level ($W=-E_F$)[91]. For physically adsorbed graphene with very weak interaction so that its electronic structure remains unchanged, W should

be related to Fermi level shift:

$$\Delta E_F = W - W_G.$$

Where W_G is the work function of freestanding graphene. We can see that although expression has a large separation between graphene sheet and metal surface for $d = 5.0$ Å, there is a small deviation ~ 0.08 eV when the equilibrium separation $d \approx 3.3$ Å, which can be traced back to the disturbance of physical adsorption of graphene, which cannot be described as a rigid offset and it can ignore this small disturbance.

Because W_G and W_M are different, if two systems communicate, electrons will transfer to balance the Fermi level. The charge transfer between metal and graphene leads to the formation of interface dipole layer and the related potential step. Once ΔE_F is determined, it can be used to obtain the work function W.

This model describes the interaction of graphene and metal and the work function shift in grapheme-metal system.

In addition to the charge transfer mechanism, the exciton-plasmon energy coupling is also considered an effective approach to enhance the detection sensitivity of SPR sensors in 2D materials-metal system[78,92,93]. The strong coupling between excitons and plasmons in 2D materials resulting in exciton-plasmon hybridization, thereby improving the detection sensitivity of SPR sensors.

Firstly, electromagnetic enhancement occurs when the exciton resonance energy of a 2D material matches the SPR energy, leading to a strong coupling effect. This is manifested as the appearance of two new, separated peaks (i.e., Rabi splitting) in the spectrum, representing new quasiparticles-plasmon polaritons (plexcitons). This hybrid state more strongly confines electromagnetic energy to the 2D material layer and its surface region. The plasmon of the noble metal film provides significant field enhancement, while the exciton further "focuses" the energy within the atomically thin 2D material plane. This means that the electromagnetic field intensity in the sensitive area of the sensor is greatly amplified. In this case, when the analyte (such as a biomolecule) is adsorbed onto the surface of the 2D material, the local RI change it induces occurs in such a strong electromagnetic field environment[94]. Therefore, the enhanced electromagnetic field "amplifies" the small RI change into a large, easily detectable spectral signal shift.

Secondly, the interface interaction is enhanced. Few-layer 2D materials possess extremely high specific surface area, abundant dangling bonds, and active surface chemical properties, making them easy to functionalize and efficiently capture target molecules. They are inherently excellent "molecular capture layers". The characteristics of excitons in 2D materials (energy, intensity, lifetime) are extremely sensitive to their surrounding dielectric environment (i.e., whether there is molecular adsorption)[95]. Even the adsorption of a single molecule can perturb the excitonic state. Additionally, in composite structures, the adsorption of molecules first directly modulates the excitons themselves (for example, leading to excitonic resonance red shift or quenching). Subsequently, this modulated excitonic state efficiently modulates the plasmonic resonance state through coupling. This is equivalent to adding a "signal amplifier": molecular adsorption to excitonic change (via coupling) to significant plasmonic change. Traditional SPR is a one-step process of "molecular adsorption to plasmonic change", whereas here it is a two-step process, with the second step playing an amplifying role.

It is particularly noteworthy that, beyond its direct impact on detection sensitivity, the coupling effect can narrow the full width at half maximum (FWHM) of the resonance peak in certain coupling modes. A sharper resonance peak implies that the shift in peak position (dip) is more easily and precisely identifiable and measurable when displacement occurs, significantly enhancing the SNR and detection accuracy (Figure of Merit, FOM) of the sensor. This makes it possible to detect extremely weak signals.

Both theoretical and experimental evidence have confirmed that 2D materials and van der Waals heterostructures (vdWhs) can significantly enhance the detection sensitivity of SPR sensors[27,96]. This is primarily due to the mechanisms of charge transfer and exciton-plasmon coupling. It is important to note that vdWhs also exhibit excitonic characteristics that differ from those of 2D materials[97,98]. Moreover, the material properties of arbitrary material stacking can produce customized excitonic characteristics, making them one of the key research directions in the field of SPR sensors. In addition to altering materials to construct customized excitonic schemes, the lattice mismatch and Moiré superlattice generated in twisted bilayer structures (homojunctions or heterojunctions, such as twisted bilayer grapheme (TBG) or MoS_2/WS_2) can produce field amplification hotspots through unique mechanisms, further enhancing the performance of SPR sensors[99]. Firstly, the Moiré periodic potential field leads to uneven charge distribution, forming regions of extremely strong local electric fields. For example, the atomic-scale local strain present in TBG can alter the density of electronic states, further enhancing the local field. This restricts the extremely high field to a very small volume near the sensing region, making it sensitive to small amounts of analytes. By changing the twist angle, twisted bilayer structures precisely control the Moiré fringe periodicity, local strain field, and hotspot distribution. Thus, external electric fields or strain can further

regulate electronic behavior, optimizing the sensor's operating point and sensitivity. Additionally, twisted bilayer structures exhibit synergistic effects with plasmonic nanostructures, achieving plasmon-exciton coupling and significantly amplifying the signal. It is considered promising to achieve extremely high field enhancement and localization, potentially detecting binding events of individual biomolecules. Simultaneously, it can detect changes in RI and molecular conformation. By regulating the twist angle through an electric field, a laminated device dynamically adjusts the sensor's sensitivity and operating range.

However, this also faces some challenges. Firstly, precise control of the twist angle, large-scale preparation of high-quality and uniform twisted bilayer structures, and their integration with SPR sensing structures still pose technical difficulties. Secondly, ensuring the long-term stability and signal reproducibility of complex heterostructures in the sensing environment is crucial. Lastly, the preparation and device processing costs of such advanced materials are high, and there is still a long way to go before they can be standardized and commercialized.

Mechanism of metasurface-based enhancement in detection sensitivity

The metasurface structure can significantly improve the detection sensitivity of SPR sensor after integrating with noble metal films[100]. The enhancement mechanism mainly has three factors. The first is SPR-LSPR synergy: noble metal nanoparticles support LSPR, while continuous metal films support propagating SPR. When the distance between the two is less than 10 nm, the electromagnetic field is strongly coupled to form a hybrid mode (upper branch/lower branch mode), and a "hot spot" is generated at the nano-gap, which increases the electric field intensity by several orders of magnitude. This mechanism has been introduced when the isolated metal nanoparticles are near the metal thin film discussed above[77,101–104]. The hybrid mode after coupling has both the large detection depth of SPR and the strong localization of LSPR, which significantly expands the electromagnetic energy density of the sensing region. Secondly, the metasurface structure (such as defective silver nanoribbons and stacked nanorings) can excite Fano resonance[81,105–108], and its asymmetric line shape is due to the interference of bright mode (radiation mode) and dark mode (nonradiation mode)[109]. This kind of resonance has sharp spectral lines (FWHM) and is very sensitive to small changes in RI. High Q value directly improves the resolution of the sensor.

In metasurface structures, the phenomenon of bound states in the continuum (BIC) is also a concept that cannot be ignored. Although the research on SPR biosensing technology based on this principle is still in its initial stage, its strong vitality in the detection field has attracted widespread attention. Therefore, we believe it is necessary to discuss the positive role of this principle in the development of SPR biosensing technology. BIC is a theoretically existing special physical state that exists in the continuum but is not coupled with radiation channels[110,111]. It can be regarded as a resonance with zero leakage and zero linewidth, possessing an infinitely large quality factor Q. Obviously, perfect BIC is difficult to apply directly in reality. However, by intentionally introducing some perturbations (such as breaking structural symmetry), BIC can be transformed into quasi bound states in the continuum (Quasi-BIC)[112]. Although Quasi-BIC loses a little bit of energy, it still maintains a very high Q factor (far exceeding traditional SPR modes), and becomes observable and excitable. Therefore, it is actually Quasi-BIC that is considered to have broad prospects in the field of sensitive detection.

Firstly, it is important to note that Quasi-BIC exhibits Fano line-shaped spectra, leading to the misconception that any system exhibiting Fano line shapes necessarily satisfies Quasi-BIC. In fact, Quasi-BIC is one of the mechanisms that give rise to extremely high-Q Fano resonances. However, Fano resonances are not necessarily Quasi-BIC. For instance, a common micro-ring resonator, Fabry-Perot cavity, or Mie resonant particle can exhibit Fano line shapes as long as its resonant mode is coupled with the background channel. In such cases, the quasi-bound state behind the Fano resonance cannot be referred to as a Quasi-BIC.

Therefore, we can refer to the promotion effect of Fano resonance on SPR biosensing technology to analyze the improvement of Quasi-BIC on the sensitivity of traditional SPR sensors. Quasi-BIC brings about a qualitative leap in the following aspects: Firstly, the Quasi-BIC mode can achieve an extremely high Q factor, which is very important because this is precisely why we discuss Quasi-BIC separately. Although other Fano resonances can also achieve high Q values, they are still far less than those produced by Quasi-BIC. In theory, a perfect BIC has an infinitely large Q value, which means that its resonance peak is extremely sharp and narrow. When there is a slight change in the RI of the sensor surface, such a sharp resonance peak, even if it produces an extremely small shift, is more easily and precisely measurable, significantly improving the detection accuracy FOM and SNR. Secondly, quasi-BIC can greatly localize light energy within a very small area on the sensor surface, generating strong electromagnetic field enhancement. When the analyte (such as a biomolecule) enters this enhanced region, the interaction between the two is amplified, thereby amplifying the sensing signal. Finally, BIC and Quasi-BIC can be implemented through various platforms, including all-dielectric metasurfaces, metal-dielectric hybrid structures,

etc. This provides the possibility for customized sensor design according to different sensing requirements (such as avoiding metal absorption loss and pursuing ultimate sensitivity).

Finally, the metasurface can dynamically adjust the reflection phase through geometric parameters (such as the period of the nanocup and the orientation of the nanorods)[113], so as to adjust the resonant wavelength of the Tamm plasmon without changing the thickness of the dielectric layer[60]. At the same time, the metasurface localizes the light field at the subwavelength scale (breaking the diffraction limit), reducing the mode volume. For example, the volume of Tamm plasmon microcavity based on metasurface is smaller than that of traditional structure mode, which enhances the strong coupling between light and exciton (such as WS_2), and the Rabi splitting increases.

Preparation strategies of various nanoparticles

Nanostructures have been gradually applied to the design and application of SPR biosensors in recent years, thanks to the rapid development of nano-preparation technology[114–117]. The precise synthesis technology of metal nanostructures became the driving force to promote the breakthrough development of SPR biosensors[118–121]. By adjusting the morphology and size (such as the preparation of gold nanorods (GNR) by seed growth method, the synthesis of silver nano-triangles by photochemical reduction, etc.)[59,61,122,123], high-density electromagnetic "hot spots" can be constructed at the sensing interface to excite the ultra-strong local field enhancement effect (up to 10^4-10^6 times)[124,125].

The dimensionality of nanomaterials is defined based on the number of external dimensions at the nanoscale (typically referring to at least one dimension ranging from 1 to 100 nanometers). This classification criterion focuses on the number of directions in which electrons are restricted in their movement through space, thereby determining their unique physical and chemical properties[126].

1. Zero-dimensional nanomaterials (0D)All 3D (length, width, height) are in the nanoscale (<100 nm). The movement of electrons in all three spatial directions is restricted, which is known as "quantum dots"[127]. Their characteristic is that due to the confinement of electrons in all directions, a strong quantum confinement effect occurs, and their optical and electronic properties (such as emission color, bandgap) are strongly dependent on their size, rather than their chemical composition. For example, quantum dots of different sizes can emit light of different colors after being excited. Such as quantum dots (such as CdSe, PbS quantum dots), metal nanoparticles (such as gold nanospheres, silver nanocubes), etc.
2. One-dimensional nanomaterials (1D)Definition: Materials with 2D on the nanoscale, while the 3D is much larger than the nanoscale (micrometer or even millimeter scale)[128]. Electrons can move freely in one direction. They exhibit excellent electron or charge transport capabilities in 1D direction, while possessing a high specific surface area. Their mechanical properties are usually excellent. Examples include nanowires and nanorods (such as silicon nanowires, GNR), nanotubes (such as carbon nanotubes (CNTs)), nanoribbons, etc
3. Two-dimensional nanomaterials (2D)Only 1D (thickness) is at the nanoscale, while the dimensions of the other 2D are macroscopic[129]. Electrons can move freely within the 2D plane. They possess a large specific surface area and extremely high in-plane carrier mobility. Many 2D materials exhibit unique electronic and optical properties that differ from their bulk counterparts (such as the Dirac cone in graphene and the direct bandgap in molybdenum disulfide). Common examples include graphene (a single layer of carbon atoms), transition metal chalcogenides (such as molybdenum disulfide MoS_2 and tungsten disulfide WS_2), MXenes and black phosphorus (BP).

Production of 0D nanostructures

0D nanostructures (such as gold, silver nanospheres, etc.), due to its inherent LSPR effect, it is widely used in fields such as environmental detection, biochemical analysis, nanomedicine, etc[130–133], and are synthesized in a many ways[134–141]. The commonly used principle is to reduce the metal precursor to nanoscale particles by chemical or physical means, and control its morphology, size and dispersion[142–146]. The main synthesis methods are as follows:

1. Chemical reduction method (liquid phase method)

The liquid phase method is one of the most commonly used chemical synthesis strategies for preparing gold and silver nanoparticles (spheres). Its principle involves forming atomic nuclei by reducing metal ions in a solution, followed by controlling the growth and stabilization of the nuclei to ultimately obtain metal particles at the nanoscale.

a. Sodium citrate reduction method (turkevich method, preparation of spherical gold nanoparticles[147]):The sodium citrate reduction method is one of the most classic liquid-phase chemical reduction methods for preparing gold and silver nanoparticles. Sodium citrate serves as both a reducing agent and a stabilizer, enabling controlled reduction of metal ions and regulation of nanoparticle size/morphology. Its reduction

mechanism relies on the reducibility of carboxyl groups, while its stabilization mechanism relies on electrostatic repulsion. This method can obtain about 10 ~ 100 nm gold nanospheres and 10 ~ 80 nm silver nanospheres. In addition, this method is often used as a precursor step of seed growth method to obtain nanoparticles "seeds". The specific steps of this method, first, the aqueous solution of $HAuCl_4$ (or $AgNO_3$) with a certain concentration kept boiling, and a certain amount of trisodium citrate was added. After stirring and cooled to room temperature, the unreacted citric acid ions were removed by centrifugal cleaning to obtain gold/silver nanoparticles for use. By adjusting the concentration of sodium citrate, the size of nanoparticles can be controlled[148,149].

b. Sodium borohydride reduction method (preparation of small silver nanoparticles): Unlike sodium citrate, sodium borohydride is a strong reducing agent that can quickly reduce metal ions, but it has poor stability and requires balancing violent reactions with particle control. Therefore, when preparing silver nanoparticles using the sodium borohydride reduction method, it is necessary to control the reaction temperature and add suitable stabilizers such as sodium citrate or polyvinyl pyrrolidone (PVP) to inhibit particle agglomeration through steric hindrance and electrostatic repulsion. The specific steps of this method, firstly, rapid mixing of $AgNO_3$ with an equimolar volume of chilled reductant solution ($NaBH_4$ and trisodium citrate in deionized water) at 0°C. The excess reductant were removed by centrifugal cleaning to obtain small silver nanoparticles[150,151]. After washing with ethanol, it is dispersed in water or ethanol.

2. Photochemical method (UV reduction)Photochemical methods primarily utilize light energy to excite reducing agents or metal ions themselves, achieving controlled reduction through photogenerated radicals or electron transfer[152–155]. Common reducing agents include sodium citrate, triethanolamine, and ascorbic acid. The steps for preparing gold nanoparticles using photochemical method are as follows: first utilized an ethanolic mixture of $HAuCl_4$ and PVP contained within a cuvette. Then, a continuous wave ultraviolet (UV) source (Generally, the wavelength is in the ultraviolet range) provided illumination at selected powers. After being exposed to light for a certain period of time, gold nanoparticles are formed. Finally, the unreacted PVP were removed by centrifugal cleaning to obtain gold nanoparticles for use[156].
3. Biosynthesis (green synthesis)Green synthesis primarily refers to the method of using natural plant extracts or biomass resources as reducing agents and protective agents, replacing toxic and harmful chemical reagents in traditional chemical synthesis to prepare gold and silver nanoparticles[157,158]. The polyphenols, flavonoids, terpenoids in plant extracts, as well as aldehyde and carbonyl groups in biomass, all possess a certain degree of reducibility, capable of reducing metal ions to metal atoms. Simultaneously, macromolecules such as cellulose and hemicellulose in these natural products can provide steric hindrance effects, preventing nanoparticles from aggregating. Taking the synthesis of gold and silver nanoparticles using green tea extracts as a case in point, firstly, green tea aqueous extract was prepared by refrigerating leaves in deionized water. Extract was collected via filtration. The residual tea material was repeatedly extracted under identical conditions. Black tea aqueous extract followed analogous preparation. Ethanolic extracts utilized ethanol instead of water.

For AuNPs synthesis, mix $HAuCl_4$ and tea extract in water and adjust pH employed $NaHCO_3$ addition at ambient temperature, AuNPs were prepared. AgNPs were similarly prepared using $AgNO_3$ instead of $HAuCl_4$. Purified nanoparticles (20-50 nm) were stored in light-protected amber vials post-centrifugation[159].

In conclusion, the chemical reaction synthesis method can synthesize nanoparticles with highly uniform size and regular morphology by precisely controlling reaction parameters (temperature, pH, reducing agent/stabilizer concentration, feed ratio, etc.)[138]. High monodispersity is crucial for SPR sensors because it can generate sharp and consistent LSPR absorption peaks, improve the energy coupling efficiency between nanoparticles and precious metal thin films LSPR-SPR, and improve the SNR and reproducibility of detection signals on the basis of increasing detection sensitivity. Liquid phase chemistry is easy to produce on a large scale, with relatively low costs, and can meet the high demand for materials in the commercialization of SPR sensors. During or after the synthesis process, various stabilizers or functional molecules can be conveniently introduced. This provides great convenience for the fixation of biological probes and is the basis for improving sensor selectivity. After decades of development, its synthesis mechanism has been thoroughly studied, the experimental plan is mature and reliable, and the repeatability is strong. However, the reducing agents, stabilizers, or other ions introduced in this method during the reaction may adsorb onto the surface of the nanoparticles, making it difficult to completely remove them. These residues can occupy the binding sites of biomolecules, non-specific adsorption of interfering molecules, or cause inactivation of biological probes, thereby reducing the selectivity and sensitivity

of the sensor. Some nanoparticles prepared by chemical methods may aggregate in complex physiological environments or long-term storage, leading to SPR peak shift and broadening, which affects the stability and service life of the sensor.

For 0D nanoparticles, although the size can be well controlled, synthesizing unconventional and anisotropic 0D structures often requires more complex formulations and more stringent conditions, challenging their monodispersity. The entire process of photothermal synthesis is usually carried out in ultrapure water or organic solvents, without the need to add any chemical reducing agents or stabilizers. Therefore, the surface of the prepared nanoparticles is very "clean", avoiding all the problems caused by chemical residues, which greatly helps to reduce non-specific adsorption and improve the selectivity and sensitivity of the sensor. The surface of laser prepared nanoparticles spontaneously forms a solvation layer (such as an OH^- layer in water), which enables them to maintain long-term colloidal stability without additional stabilizers, improving the reliability of the sensor. Multiple metal nanoparticles can be synthesized by simply changing the target material[147]. For SPR sensing, gold, silver, copper, and their alloy nanoparticles can be conveniently prepared to optimize the SPR response window and intensity. The laser ablation process can be synchronized with surface modification, and by selecting different liquid environments, nanoparticles with specific functional groups on the surface can be directly synthesized. Laser ablation is an instantaneous high-energy process that is difficult to finely control nucleation and growth at a "slow" pace like chemical methods. Therefore, the size distribution of the prepared nanoparticles is usually wide (with high polydispersity), which can lead to broadening of the SPR absorption peak, which is not conducive to obtaining high sensitivity and reproducibility signals. Compared to chemical methods, laser ablation requires larger equipment investment (high-energy lasers), has relatively lower synthesis efficiency, is difficult to produce on a large scale, and has higher costs. Although size can be controlled to some extent by adjusting laser parameters (energy, pulse width, wavelength) and solvent, its controllability and predictability are not as good as chemical methods, making it difficult to achieve on-demand synthesis of specific sizes.

The biosynthetic method (green synthesis method) uses biomass resources, with mild reaction conditions (constant temperature aqueous phase)[160], no need for toxic chemicals, in line with the principles of green chemistry, extremely low cost, and sustainability. Biological templates (such as proteins and peptides) will directly coat the surface of nanoparticles while reducing metal ions. These biomolecules can naturally serve as recognition elements and can be directly used for detection, simplifying the sensor construction steps. Due to the use of biomolecules as coating layers, synthesized nanoparticles typically exhibit excellent biocompatibility and have great potential for in vivo biosensing applications. The biological molecule coating layer can provide good steric hindrance or electrostatic stability for nanoparticles. Poor monodispersity and controllability: This is the biggest weakness of green synthesis methods. The composition of biological extracts is extremely complex, and the differences in each batch lead to unpredictable reduction and stabilization abilities. Therefore, the size and morphology of synthesized nanoparticles vary greatly, and the reproducibility is extremely poor. This is a fatal disadvantage for SPR sensors that require uniform and stable signals. The surface of the particles is coated with a complex mixture of biomolecules, which may be arranged in a random manner. This not only makes it difficult to precisely control the fixed orientation and density of probe molecules, but it may also generate strong nonspecific adsorption, seriously interfering with the specific recognition of target substances and significantly reducing the selectivity and sensitivity of the sensor. The reaction mechanism involves the synergistic effects of multiple biomolecules, which have not been fully elucidated to date. This makes it difficult to standardize and precisely regulate the process, resulting in a high dependence on the source and batch of biological raw materials. Overall, if pursuing high-performance and high reliability SPR sensors, chemical synthesis method is still the most practical choice after optimization. Photothermal synthesis, as a "pure" preparation method, is a strategic direction for solving specific adsorption problems in the future, but it needs to be combined with subsequent separation and purification technologies (such as centrifugation and filtration) to improve monodispersity. The concept of biosynthetic methods is attractive, but unless breakthroughs are made in mechanism research and process control (such as using genetically engineered bacteria to produce a single reducing protein), their applications will mainly be limited to fields that do not require high signal consistency.

Production of 1D nanostructures

1D nanostructures mainly refer to nanoscale structures such as nanowires and nanorods. 1D noble metal nanostructures have received widespread attention due to their flexible and adjustable LSPR resonance frequency[161,162]. This characteristic has been widely applied in various fields, especially in biological detecting and biomedical research[163]. The preparation of 1D gold and silver nanorods/wires primarily employs the

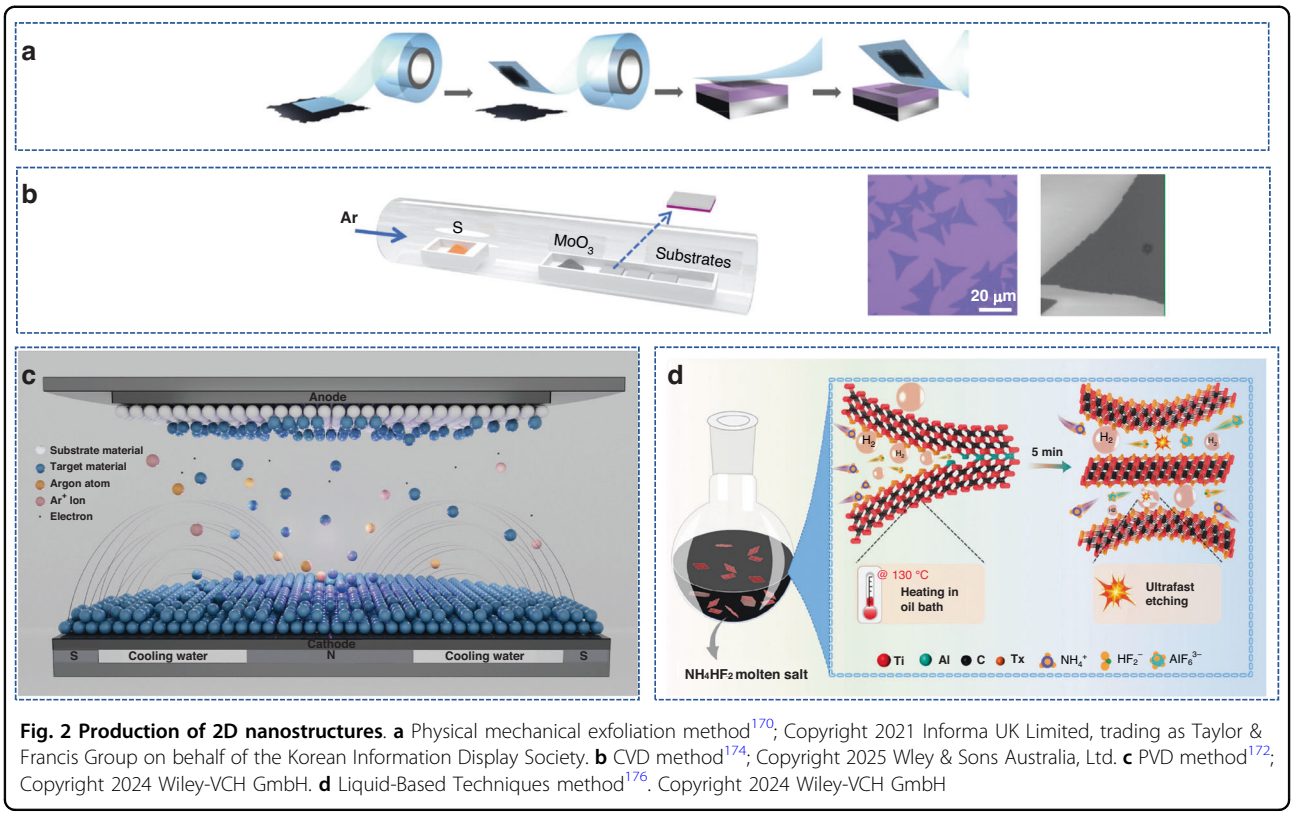

Fig. 2 Production of 2D nanostructures. **a** Physical mechanical exfoliation method[170]; Copyright 2021 Informa UK Limited, trading as Taylor & Francis Group on behalf of the Korean Information Display Society. **b** CVD method[174]; Copyright 2025 Wley & Sons Australia, Ltd. **c** PVD method[172]; Copyright 2024 Wiley-VCH GmbH. **d** Liquid-Based Techniques method[176]. Copyright 2024 Wiley-VCH GmbH

seed growth method[164], utilizing hexadecyltrimethylammonium bromide (CTAB) as a template. By regulating the growth of gold and silver nanoparticles (with growth proceeding on a seed-based foundation), the aspect ratio of the nanorods can be modulated, thereby tuning their plasmonic resonance properties. The CTAB concentration is a crucial determining factor. Reducing agents commonly used include ascorbic acid (AA) and sodium borohydride. The preparation of gold/silver nanorods via the seed growth method: Firstly, preparation of seed solution: Add $HAuCl_4 \cdot 3H_2O$ aqueous solution to CTAB solution in a test tube (glass or plastic). The solution is gently mixed by reversing and the color is bright brown yellow. Then, immediately add cold $NaBH_4$ aqueous solution, and then quickly reverse the mixing. It should be noted that the escaping gas is allowed to escape during the mixing process. The tubes were then stored in a water bath for future use. The seed solution can be used for more than 1 week.

Secondly, preparation of GNR: Take an appropriate amount of CTAB solution, water, $HAuCl_4$, $AgNO_3$, L-ascorbic acid and seed solution, remove them one by one in the test tube according to the given order, invert and gently mix. For example, CTAB, $HAuCl_4 \cdot 3H_2O$ and $AgNO_3$ solution were added to the test tube in sequence, and then gently mixed by inversion. The solution at this stage exhibits a bright brownish-yellow color. Upon subsequent addition of L-ascorbic acid, the solution turns colorless after thorough mixing. Finally, add seed solution, gently mix the reaction mixture and let it stand for at least 3 h[165–167].

Production of 2D materials

2D materials are synthesized through diverse methodologies, encompassing mechanical exfoliation, physical vapor deposition/transport (PVD/PVT), chemical vapor deposition (CVD), and solution-phase techniques[96,168].

1. Physical mechanical exfoliationPhysical mechanical exfoliation employs adhesive tapes to isolate atomically thin layers from bulk crystals[169,170]. It enables the production of both monolayer 2D materials and custom vdWhs, finding increasing application in surface plasmon resonance (SPR) sensors. The process involves: (i) isolating monolayers via sequential cleavage, (ii) transferring exfoliated flakes onto target substrates (e.g., quartz, SiO_2/Si), and (iii) for heterostructure fabrication, precisely stacking monolayers with controlled twist angles (as shown in Fig. 2a. Interlayer cohesion in these heterostructures arises solely from vdW interactions.
2. Physical vapor deposition/transport (PVD/PVT) PVD or PVT refers to technology where in a vacuum environment[171,172], vaporize source

materials into atomic, molecular, or ionic species, subsequently condensing them onto substrates (as shown in Fig. 2b. Precise control over pressure, source material, and deposition parameters is critical for obtaining high-quality thin films.

3. Chemical vapor deposition (CVD)Chemical vapor deposition (CVD)[173,174] recognized as the benchmark method for controlled synthesis of 2D materials and their heterostructures. This method facilitates precise modulation of growth orientation and crystallinity (as shown in Fig. 2c. Its major advantage lies in the ability to sequentially grow distinct 2D materials atop one another, forming heterostructures with atomically clean interfaces and minimal impurity incorporation.
4. Liquid-Based TechniquesIn addition, Liquid-based exfoliation has emerged as a scalable platform for 2D material production, enabling applications in printed electronics and additive manufacturing[175,176].

Ultrasonication of layered precursors in solvents generates inhomogeneous stress, leading to layer separation via pin-hole formation. For air-sensitive materials like BP, stability during processing is enhanced by: (i) surfactant addition or (ii) thermal exfoliation in high-boiling-point solvents matching the material's surface energy. Challenges in controlling film thickness, lateral dimensions, and surface chemistry often necessitate post-processing for improved monodispersity (as shown in Fig. 2d. Alternatively, ion intercalation precedes mild sonication to weaken interlayer bonding in bulk crystals, yielding larger, higher-quality flakes[177]. However, this method chemically modifies the material, altering its intrinsic properties, making it suitable for specific application-driven syntheses.

The physical mechanical exfoliation method can produce 2D nanosheets with complete crystal structure, minimal defects, and clean surface. This is crucial for SPR sensors, as defects can introduce non radiative recombination centers, weaken signal enhancement effects, and may lead to non-specific adsorption. The non-destructive lattice ensures the intrinsic and excellent optical and electrical properties of the material, such as the high carrier mobility of graphene, which facilitates efficient plasma exciton coupling or charge transfer, thereby achieving maximum sensitivity enhancement. The process does not involve any chemical reactions, and the obtained nanosheets are very pure, avoiding interference from impurities in the biological recognition process and improving selectivity. The extremely low yield and lack of regulatory modeling are the most fatal drawbacks of this method. The process is cumbersome and highly random, making it difficult to obtain thin films of sufficient size and uniform thickness to cover standard SPR chips, which seriously hinders its application in practical sensors. The size, thickness, and shape of each peeled layer are inconsistent, resulting in significant differences in the performance of sensors based on different chips, making it difficult to ensure reproducibility and almost impossible to standardize production. Accurately and non-destructively transferring micrometer scale peeled thin films to specific locations on SPR chips is a huge technical challenge that is difficult to achieve automated integration. It is mainly used for basic mechanism research to verify the theoretical upper limit of the improvement of SPR performance by 2D materials themselves, but it is almost impossible to use for large-scale manufacturing of actual sensor devices.

PVD (especially sputtering) is very suitable for depositing large-area, uniformly thick continuous thin films (such as metal or dielectric layers of several nanometers) on flat substrates. This highly matches the requirement of uniform coating for SPR chips. Sedimentary particles have high energy, forming a thin film and not easily detached, improving the mechanical stability and service life of the sensor. The vacuum environment avoids pollution, and by precisely controlling the time, and substrate temperature, the film thickness can be well controlled, which is a key parameter for regulating SPR signals. PVD is a standard process in the semiconductor industry that is easy to integrate with other micro-nano processing technologies, laying the foundation for manufacturing miniaturized and arrayed SPR sensors. 2D polycrystalline films prepared by PVD, such as polycrystalline graphene, have more grain boundary defects. Grain boundaries scatter plasma and charge carriers, reducing sensor performance and potentially becoming non-specific adsorption sites. Mainly used for preparing graphene or simpler metal oxides, for complex transition metal dichalcogenides (TMDs) and other compounds, it is difficult to accurately control the stoichiometric ratio, and the material quality is usually lower than that of CVD method. Expensive vacuum equipment is required, resulting in higher costs. It is an ideal choice for preparing ultra-thin metal protective layers (such as sputtering a layer of ultra-thin graphene on silver film to prevent oxidation) and uniform dielectric reinforcement layers, which are very suitable for standardized and large-scale production of SPR sensor chips. CVD is the most mainstream method for preparing large-area, high-quality, and single crystalline 2D materials, especially graphene and TMDs. Its material quality is much higher than PVD and liquid-phase methods, close to mechanical exfoliation, while also having the potential for scaling up. By optimizing the catalyst, temperature, airflow, and reaction time, precise and controllable growth of single or specific layers can be achieved, which is crucial for finely regulating the sensitivity and operating range of SPR sensors. There are various types of 2D materials that can be prepared, including graphene

h-BN、 Multiple TMDs and their heterojunctions provide the possibility to customize SPR sensors for different detection requirements, such as different laser wavelengths. Growth is typically carried out on rigid substrates such as copper foil and SiO_2/Si at high temperatures (>800°C). Afterwards, the grown film needs to be transferred onto an SPR chip (usually glass or prism). The transfer process is prone to introducing wrinkles, cracks, contamination, and defects, seriously deteriorating material performance and sensor reproducibility. The equipment is expensive, the process parameters are complex, the requirements for operators are high, and the overall cost is higher than PVD and liquid-phase methods. The interface contact quality and adhesion between the transferred 2D material and the metal film of the SPR chip may not be as good as the film deposited directly by PVD, which may affect stability and thermal management. It is one of the preferred methods for preparing high-performance and high-end SPR sensors. Despite the transfer challenges, the high-quality materials it provides are irreplaceable for applications that pursue extreme sensitivity. Solving non-destructive transfer technology is a key research direction.

The liquid-phase synthesis method has a simple process, low equipment requirements, and can produce 2D material dispersions on a large scale, with significant cost advantages[175,178]. The obtained nanosheet dispersion can be easily and quickly coated onto SPR chips of any shape and material through various methods such as spin coating, droplet coating, spray coating, Langmuir Blodgett self-assembly, etc., without the need for high temperature and transfer steps, making integration simple. During or after the liquid-phase exfoliation process, it is convenient to perform covalent or non-covalent chemical modifications on the nanosheets, directly attaching biometric molecules to achieve material preparation and functionalization in one step. Liquid phase exfoliation can produce nanosheets with high defect density, small lateral dimensions, and uneven layers. Serious defects and edges will significantly weaken its optoelectronic performance and introduce a large number of non-specific adsorption sites, severely reducing the selectivity and SNR of the sensor. Thin films coated by solution method are usually randomly stacked from nanosheets, which have problems such as pores and non-uniformity, resulting in uneven SPR response and poor reproducibility. The solvents or surfactants used may be difficult to completely remove, and residues can contaminate the sensor surface and interfere with biometric recognition. Very suitable for disposable SPR sensors or test paper products with low performance requirements and extreme cost sensitivity. Strict centrifugal screening and subsequent processing can partially improve material quality, but breakthroughs are still needed to apply it to high-precision detection.

Production of metasurfaces

Metasurfaces are 2D artificial materials composed of nanostructures, which can accurately control the phase, amplitude and polarization of electromagnetic waves (light, microwave, etc.)[50]. The preparation methods are various, and the appropriate process should be selected according to the material system (metal, medium, composite) and the target function (holography, lens, polarization control). The main preparation methods and detailed steps are as follows:

1. Electron beam lithography (EBL)Electron Beam Lithography (EBL) is one of the core technologies for fabricating optical metasurfaces. It achieves precise processing of sub-wavelength structures by directly writing nano-patterns on a resist through focused electron beams, combined with subsequent pattern transfer processes (as shown in Fig. 3a. The general steps mainly include substrate preparation, coating, electron beam exposure, development, pattern transfer, and post-processing: Silicon wafers or glass substrates were subjected to successive ultrasonic cleaning in acetone, isopropanol, and deionized water, with subsequent drying using nitrogen gas. An SU-8 2000 photoresist formulation was spin-coated onto substrates, yielding uniform nm-thick films. Pre-exposure baking was performed on a hotplate. Post-exposure baking was intentionally omitted to minimize residual layer formation and prevent thermally induced crosslinking, thereby preserving feature dimensions. Exposed samples were developed at ambient temperature through sequential immersion in: (i) Propylene glycol monomethyl ether acetate, (ii) Isopropanol, (iii) Flowing deionized water rinse. Patterned substrates were dried under a nitrogen stream. Metal nanostructures were obtained by metal deposition and stripping (acetone ultrasound)[179].
2. Focused ion beam (FIB)FIB is a technology that utilizes focused ion beams for material processing at the nanoscale. Its core principle involves bombarding the material surface with ion beams (usually gallium ions) focused to nanometer-sized dimensions, removing material through physical sputtering effects. The general steps for fabricating metasurfaces using FIB mainly include: First, substrate preparation: deposit the target material film (such as 30 nm gold film) on the silicon substrate. Second, ion beam etching: import design patterns into FIB system, select ion source (such as Ga^+), set beam current and acceleration voltage.

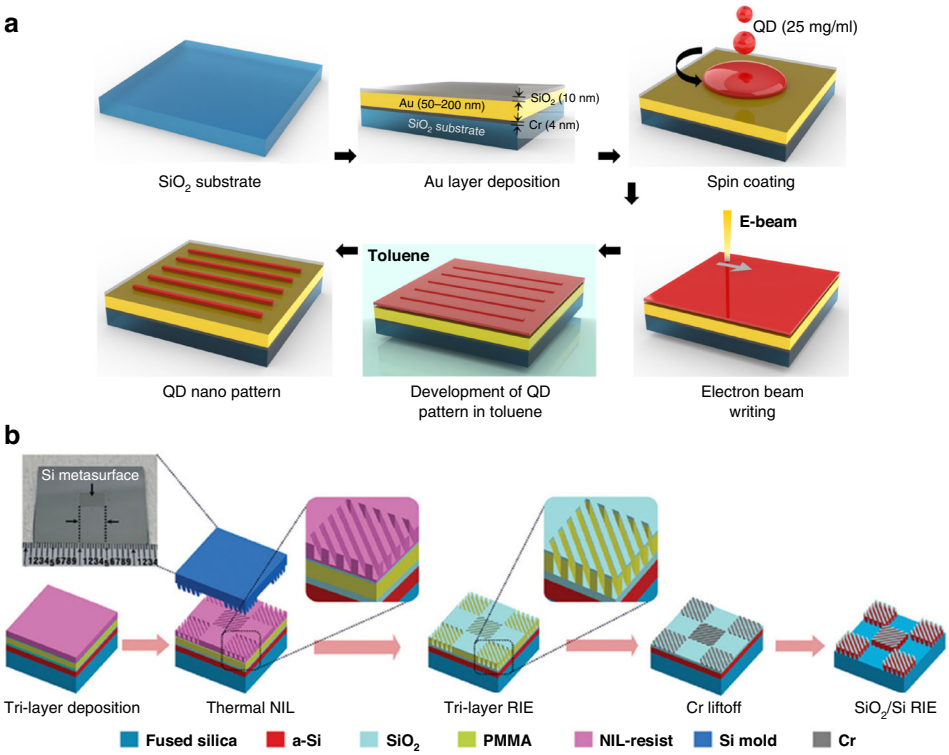

Fig. 3 Production of metasurface. **a** EBL method[49]; Copyright 2025 De Gruyter Brill. **b** NIL method[181]. Copyright 2024 Wiley-VCH GmbH

Direct scan etching removes excess metal and forms nanostructures. Third, Cleaning and characterization: the residue was removed by argon ion polishing, and the structural morphology was examined by scanning electron microscope (SEM)[180]. The core of fabricating FIB-induced metasurfaces lies in the synergistic regulation of physical sputtering and stress deformation, achieving sub-wavelength structure customization through a process of "2D etching → selective bombardment → three-dimensional transformation".

3. Nanoimprint lithography (NIL)The principle of nanoimprint technology is mechanical imprint transfer of patterns. It utilizes a mold with nanoscale patterns (usually fabricated through electron beam lithography) to imprint patterns on a substrate coated with resist or other moldable materials. Unlike optical lithography, NIL is not restricted by the diffraction limit, thus enabling higher resolution. Its general process includes (as shown in Fig. 3b): Initially, coat the thickening agent on the cleaned silica chip and subsequently heating on a heating plate. The UV-NIL resist was then coated onto the substrate, followed by UV-NIL using the fabricated fused quartz vertically coupled double-layer gratings (VCDG) mask aligner. Once the calibration is verified, UV exposure is used to crosslink the resist, and optical performance of the cured resist becomes a polymer similar to SiOx. UV resist has low viscosity and is easy to fill during nil to achieve high fidelity pattern transfer at relatively low pressure. After UV-NIL, a mild oxygen plasma process was used to treat the printed resist scaffolds to activate the hydroxyl groups on the surface. Evaporate a layer of Cr, and then deposit Al to form VCDG grating. The high vacuum level helps to obtain a smoother VCDG surface morphology by reducing the residual gas and pollutants in the chamber. Finally, a SiO_2 layer was deposited as a packaging layer to avoid further oxidation of the aluminum surface[181].
4. Self-assembly technologySelf-assembly is a technique that utilizes intermolecular forces to spontaneously and orderly arrange structures to prepare regular patterns. The application of self-assembly technology in the fabrication of metasurfaces involves designing and controlling the weak interactions between nano/molecular "building blocks" and their interactions with the environment (especially the substrate), guiding these building blocks to spontaneously and large-scale arrange into stable and ordered structures with desired sub-

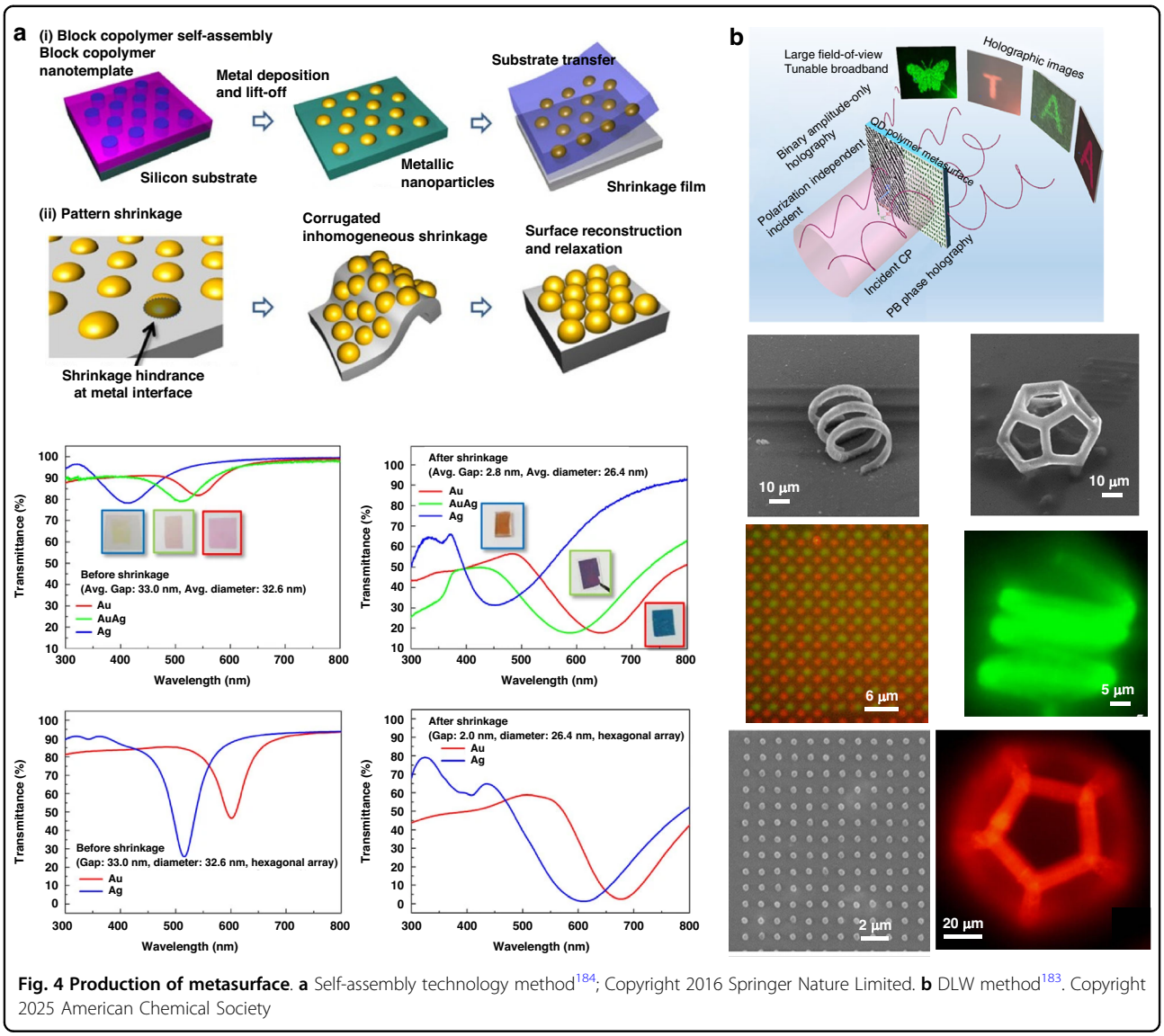

Fig. 4 Production of metasurface. **a** Self-assembly technology method[184]; Copyright 2016 Springer Nature Limited. **b** DLW method[183]. Copyright 2025 American Chemical Society

wavelength features and spatial configurations, thereby achieving optical functions of metasurfaces. It primarily relies on non-covalent interactions (such as π-π stacking, etc.) between molecules, nanoparticles, or larger structural units. These interactions are relatively weak but possess directionality and selectivity. Generally, the preparation of metasurfaces using self-assembly technology involves two main steps (as shown in Fig. 4a: First, gold nanoparticles were synthesized by redispersion in deionized water. Second, Silicon/glass substrates were functionalized with sequential Cr adhesion and Au films via magnetron sputtering. These Au-coated substrates were immersed in colloidal dispersion for controlled durations. Electrostatic self-assembly occurs due to the negative surface charge inherent to sputtered Au films, which attracts functionalized Au nanoparticle (positive charge). Consequently, metasurfaces comprising Au film-coupled Au nanoparticle were fabricated. The surface coverage density was precisely modulated by varying immersion time, enabling tunable optical properties[182].

5. Direct laser writing (DLW)Laser direct writing is a technique that utilizes computer-controlled high-precision laser beam scanning to directly expose and write any designed pattern on photoresist (in Fig. 4b. The core principle is to achieve precise fabrication of micro-nano structures by utilizing the interaction between laser and materials (such as photopolymerization, ablation, phase transition, etc.). The key processes include: First, Photoresist coating: spin the photoresist (such as SU-8) on the substrate with a thickness of 1–10 μM. Second,

Laser exposure: femtosecond laser focused scanning, curing colloid through two-photon polymerization. The design path is controlled by CAD software. Third, Development and metallization: the developer removes the unexposed area to obtain the polymer structure. Sputter metal (such as aluminum) to form a conductive metasurface[183].

In conclusion, EBL has the highest resolution (up to several nanometers) and can process metasurface units with extremely complex shapes and extremely small feature sizes. This provides the possibility for designing high-performance resonance modes, such as supporting local surface plasmon LSPR and surface lattice resonance (SLR) coupling, greatly improving the sensitivity and quality factor (FOM) of sensors[179]. No mask is required, and exposure can be directly based on digital design graphics, which is very suitable for scientific research exploration and prototype verification. Gradient, non-uniform, and encoded metasurfaces can be easily implemented for multifunctional integration, such as simultaneous detection of RI and thickness. The ability to achieve highly consistent structures on a single chip ensures high reproducibility of sensor response, which is crucial for quantitative analysis. Electron beam point-by-point scanning exposure is very slow and not suitable for large-scale production, only suitable for laboratory small-scale preparation. The expensive equipment, high maintenance costs, and complex process (requiring ultra-vacuum environment, etc.) result in extremely high preparation costs for individual chips. Electron scattering can cause unexpected exposure of the resist in non-target areas, affecting the processing fidelity of complex and dense patterns, requiring compensation through algorithms and increasing process difficulty.

FIB can directly engrave metasurface structures on metal thin films without the need for resist and pattern transfer processes. This makes it the fastest method for prototyping single devices/small arrays, making it very suitable for rapid iterative design. Similar to EBL, it has nanometer level machining accuracy, can process any 2D shape, and can be flexibly modified and edited. By controlling the ion beam dose and angle, superatomic particles with 3D contours can be created, providing more degrees of freedom for phase control. Similarly, point by point scanning is even less efficient than EBL, and the equipment is also expensive, making it unsuitable for large-scale production. High energy Ga^+ ions can be injected into the sample, altering the lattice arrangement and photonic properties of the material, resulting in broadening of the SPR resonance peak, thereby reducing the sensitivity and SNR of the sensor. This is a fatal flaw for high-performance sensing. Usually, it can only process a very small range, making it difficult to prepare large-area uniform metasurfaces.

NIL, once the master is made, can replicate nanostructures at high speed and in large quantities like "stamping", with a large single imprint area. This is the most promising path to achieve low-cost and commercial mass production of metasurface SPR sensors. The ability to perfectly replicate the nano features of the master plate, with high resolution and excellent batch consistency, ensures high reproducibility of sensor products. It can be processed on substrates such as glass, silicon, and even flexible polymers, providing the possibility for developing flexible and wearable SPR sensors. The production of large-area, defect free nanoimprint master plates requires expensive technologies such as EBL, and the master plates are prone to wear and contamination. Etching errors (multi-layer alignment), uneven filling of resist, and demolding defects can introduce processing defects, affecting the consistency of yield and sensor performance. The optical properties of the imprinting adhesive may not be ideal, and it is usually necessary to use it as a mask and then transfer it to functional materials, which increases the complexity of the process.

Self-assembly is a bottom-up process that allows for parallel formation of nanostructures over a large area, at a much lower cost than any top-down photolithography technique[184]. Especially with self-assembly, nanolattices or pore arrays with feature sizes<10 nm and extremely high densities can be easily prepared for exciting ultra-sharp resonance modes, which is expected to achieve extremely high sensitivity. In theory, nanostructures can be formed on complex surfaces. Limited structural design and controllability: The types of structures formed are limited by thermodynamic equilibrium states, making it difficult to arbitrarily design complex shaped superatoms and limiting the ability to control optical responses. Long range orderliness problem: self-assembly usually produces polycrystalline domains, which are ordered within domains but have grain boundaries and defects between domains. This can lead to uneven SPR response and poor reproducibility, which is a major obstacle to sensing applications. Process integration and reliability: It is difficult to integrate self-assembled materials with standard complementary metal-oxide-semiconductor (CMOS) processes, and the thermal and mechanical stability of the structure is sometimes poor. It has potential in specific and simple sensing applications, such as SERS detection that requires low consistency of ultra-high density hotspots.

DLW is the only option for creating 3D metasurfaces. Complex 3D structures such as suspended and stacked structures can be constructed, providing a platform for achieving richer light field control, thus developing new SPR sensing modes. Similar to EBL, it belongs to digital direct writing technology and is suitable for prototype development. The resolution can break through the

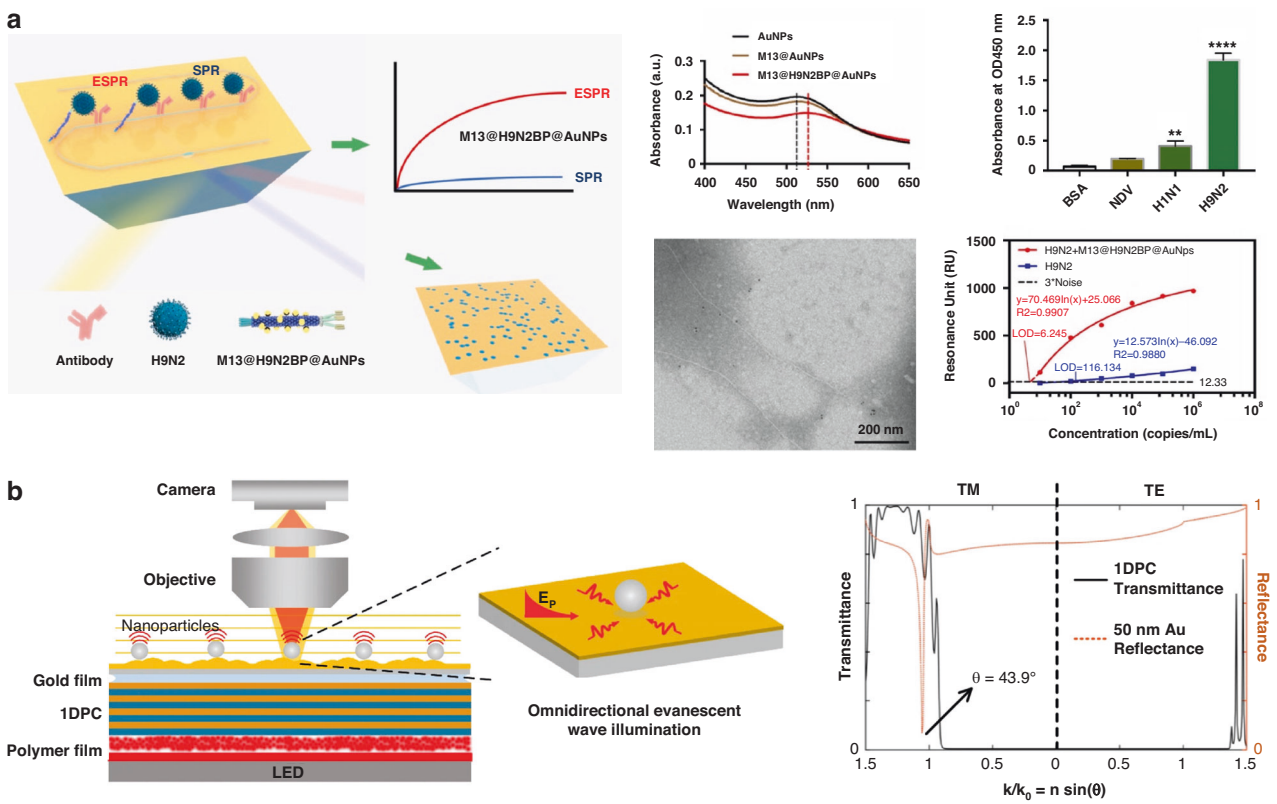

Fig. 5 SPR biosensors based on Metal film and 0D nanoparticles a Detection principle of virus particles (H9N2) with phage@AuNPs nanofibers serving as probes[201]. Copyright 2023 Elsevier B.V. All rights reserved. **b** Experimental configuration of Chip-PSM utilizing an upright microscope[202]. Copyright 2025 Springer Nature Limited

diffraction limit and reach the level of hundreds of nanometers. Although it is a parallel process (two-photon absorption), it still scans point by point, which is slow and not suitable for large-scale production. Usually, polymer templates are processed first, and subsequent metallization steps (such as magnetron sputtering) are required to form plasmonic metasurfaces. The shape retention and surface roughness of metal coatings can affect the final performance. Besides, femtosecond laser systems are expensive. But it also is the core technology for developing the next generation of 3D SPR metasurface sensors. Used to explore sensing mechanisms based on new dimensions such as angular momentum and orbital angular momentum, but currently mainly in the laboratory research stage.

Recent progress of SPR biosensors using composite nanostructures

The breakthrough significance of composite nanostructured SPR biosensor lies in the collaborative jump of multi-dimensional performance, which completely innovates the detection limit and application boundary of traditional single metal film. Firstly, the detection sensitivity breaks through the physical limit. Through charge transfer and multiple resonance coupling, the local electric field is enhanced by 10^4 to 10^6 times, and the detection limit is below pM level[185,186]. SPR biosensors sensitized by nanostructures have found extensive application in cutting-edge fields such as single molecule cancer marker screening, corrosion-resistant all carbon sensors, robot tactile fusion, chemical mechanical sensing and so on[187–191]. It has greatly promoted SPR from laboratory to high-tech industries such as precision medicine and intelligent Internet of things.

Metal thin film structure has always been the core component of SPR biosensor[192–194]. The SPR biosensor designed in cooperation with nanostructure has made rapid progress in recent years through plasmonic hybridization and interface quantum effect[195,196], and constantly broke through the performance limit.

Metal film and 0D nanoparticles

The SPR biosensor based on metal nanofilm combined with 0D metal nanoparticles is one of the important studies in this field, and has achieved numerous results so far, gradually occupying a very important position in

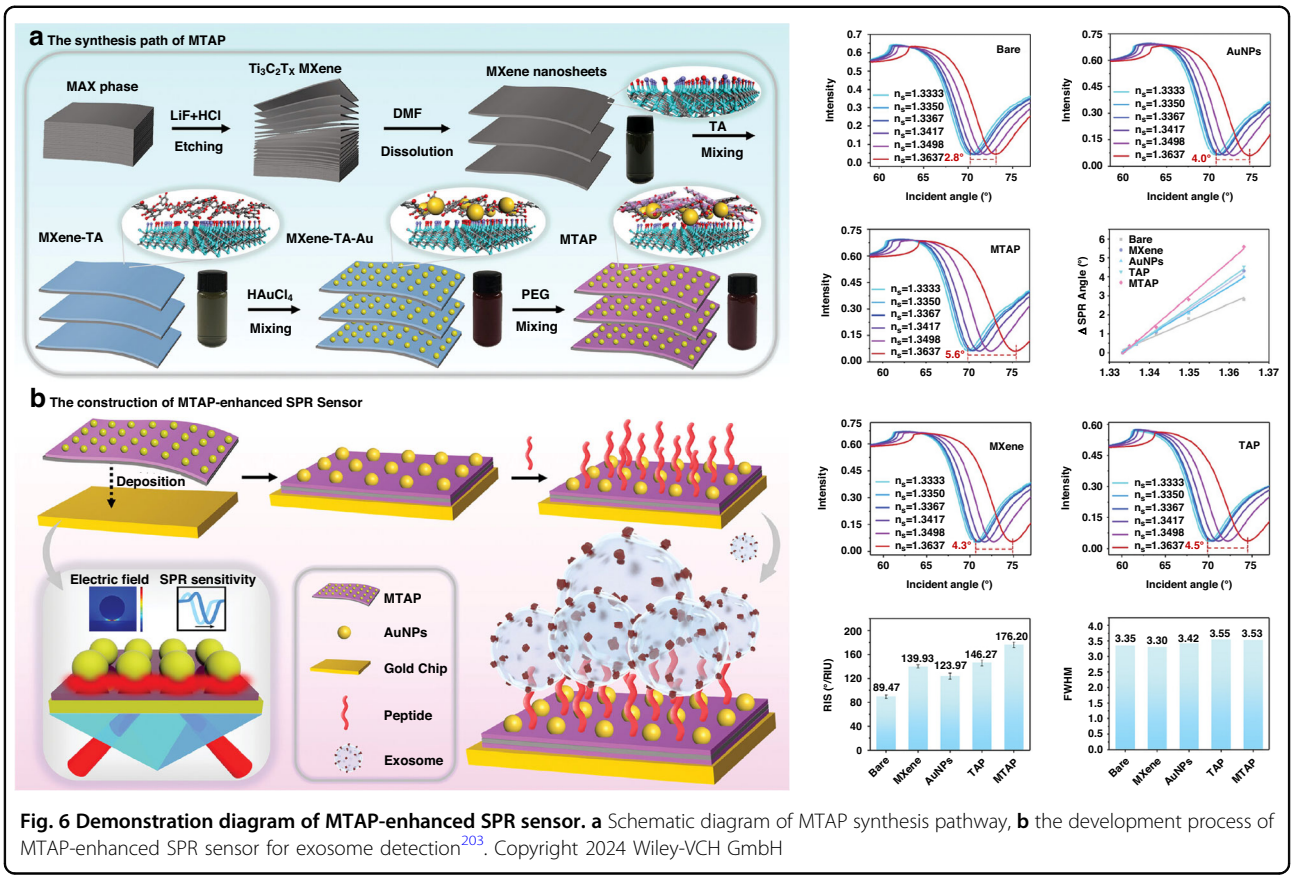

Fig. 6 Demonstration diagram of MTAP-enhanced SPR sensor. a Schematic diagram of MTAP synthesis pathway, **b** the development process of MTAP-enhanced SPR sensor for exosome detection[203]. Copyright 2024 Wiley-VCH GmbH

practical applications[151,197–200]. Based on the SPR-LSPR coupling effect between metal nanospheres and metal thin films, Hou et al. recently engineered a sensitive SPR biosensor for rapid detection of avian influenza H9N2, demonstrating exceptional analytical performance[201]. Simulation modeling shows a 40-fold electric field enhancement at the SPR interface compared to conventional AuNP-functionalized sensors (as shown in Fig. 5a. Experimental validation achieved a detection limit of 1.04×10^{-5} fM for H9N2 in allantoic fluid, with acquisition times under 10 min. A distinctive feature involves post-capture conversion of bound phage nanofibers into quantifiable plaques. This secondary quantification modality enables direct viral enumeration, providing orthogonal validation of SPR results through plaque counting.

In response to the problems of low spatial resolution and limited field of view in traditional surface plasmon microscopes (SPRM), You et al. introduced a compact, large field of view surface plasmon scattering microscope (PSM)[202]. In comparison to traditional SPRM, PSM preserves a better detection performance of in situ label-free analysis, a broader field of view and higher spatial resolution (as shown in Fig. 5b. This technology has been successfully applied to the detection of nanoparticles and biological samples, and it is considered to have broad application prospects in the fields of molecular dynamics and chemical reaction process research.

Utilizing the plasmonic coupling effect, and combining the charge transfer mechanism between 2D materials and gold films, Wang et al. provided a novel 2D semiconductor/0 d plasmon heterojunction MXene TA Au PEG (MTAP) as a high-performance and multifunctional photovoltaic interface material (as shown in Fig. 6)[203]. MTAP can not only effectively protect MXene from accumulation and spontaneous oxidation, but also has excellent photoelectric performance and interface antifouling ability. In addition, MTAP was used to enhance SPR spectrum, allowing direct and real-time detection of tumor cell exosomes with limit of detection (LOD) of 0.28 mL^{-1}. MTAP effectively meets the requirements of sensitivity, specificity and stability of the sensor by integrating the characteristics of photoelectric enhancement, interface antifouling and oxidation stability. Finally, the results of serum sample analysis show that the sensor has a certain potential application value in clinical diagnosis.

Additionally, Lin et al. put forward a novel approach for the detection of miR-183 associated with BC and miR-155 microRNAs using pH responsive triple DNA nanoswitch (TDN) based on plasmonic coupling mechanism[204]. This stepwise SPR biosensing platform enables sequential

detection of dual miRNAs through pH-modulated signal transduction. The sensing interface features two immobilized triple-helix molecular switches (SA and SB), anchored via hybridization between SA/miR-183 and SB/miR-155 complexes to s9.6 antibody-functionalized surfaces. Streptavidin-conjugated Au nanoparticles tethered to biotinylated reporter chains serve as amplification tags, generating concentration-dependent SPR reflectivity shifts upon pH-induced displacement: miR-183 detection at pH 5.0 (LOD: 0.57 pM) and miR-155 detection at pH 8.3 (LOD: 0.83 pM). Clinically validated in urine analysis, the platform distinguished breast cancer patients from healthy controls. Its modular design permits adaptation for detecting other disease-relevant miRNA pairs non-invasively.

Serum leukocyte chemokine-2 (LECT2) has emerged as a clinically significant biomarker for liver fibrosis diagnosis. Therapeutic targeting of the LECT2/Tie1 signaling axis shows considerable promise for novel treatment strategies. Despite this potential, current methodologies for ultrasensitive quantification of circulating LECT2 remain constrained. SPR offers label-free biomolecular interaction analysis through RI monitoring. While SPR technology demonstrates exceptional biomarker sensitivity, achieving direct LECT2 detection at clinically relevant levels presents substantial analytical challenges. Combining the plasmonic coupling between nanoparticles and metal films, as well as the charge transfer mechanism between molybdenum disulfide and gold films, Zhou et al. proposed a novel enhanced SPR biosensor addressing the limitations of existing LECT2 detection methods (as shown in Fig. 7)[205]. MoS_2 nanosheets can provide isolated contact between Au thin films and cyclodextrin functionalized AuNPs (CD AuNPs), thereby forming a gap mode plasma structure. This design substantially amplifies near-field electric field intensity at the Au film interface, enhancing RI detection sensitivity. Compared to conventional Au-film SPR sensors, our optimized platform demonstrates an 82% sensitivity enhancement (from 73.1 to 133.3 deg/RIU) with superior FOM and detection accuracy. A TFF-labeled peptide was specifically immobilized through host-guest interactions within CD hydrophobic cavities. This functionalization enabled ultrasensitive quantification of liver fibrosis biomarker LECT2, achieving a wide dynamic range with 0.62 ng/mL detection limit.

Combine 0D nanoparticles and metal film structure are one of the most important directions in SPR biosensing technology research. The classical liquid-phase synthesis method can facilitate the synthesis of spherical gold/silver nanoparticles, as well as anisotropic particles such as nanocubes and nanostars to produce stronger LSPR. This type of nanomaterial synthesis technology is mature and has good monodispersity. Nanoparticles with high specific surface area increase the fixed density of biometric elements such as antibodies and aptamers. Therefore, the manufacturing strategy combining solution-based synthesis of nanomaterials with self-assembly/spin coating technology provides the best cost-effectiveness balance. Other synthesis methods, such as electrostatic self-assembly, chemical bonding (fixing AuNPs on gold films through bifunctional molecules), and in-situ growth (directly growing nanoparticles on thin films through seeds), have greatly expanded the application prospects of metal nanofilm/0D nanoparticle composite structure SPR biosensors as effective supplements to this type. Under current technological conditions, this solution is currently the mainstream application and has been widely used in various fields.

Metal film and 1D material

1D metal nanostructure is a nanoscale (usually 1~tens of nanometers) nanostructure with a length of up to micron, which has high aspect ratio and significant quantum confinement effect. Its distinctive physicochemical characteristics encompass high electrical conductivity, excellent flexibility, SPR effect and high specific surface area, which are widely used in the design of SPR biosensors.

When 1D nanorods/wires are close to metal thin films, they also exhibit a plasmonic coupling mechanism, which can significantly enhance detection sensitivity. In addition, 1D nanorods can achieve precise control of plasmon resonance frequency by adjusting their aspect ratio, maximizing detection performance. Recently, based on this principle, Tan et al. introduced a novel configuration where frequency-shifted light beams of distinct polarizations are retroreflected into the laser cavity to induce laser heterodyne feedback interferometry[206], which amplification strategy enhances reflectivity modulation from RI variations at the gold-coated SPR interface. S-polarized light serves as an intrinsic reference channel, effectively compensating system noise. The optimized platform achieves an RI resolution of 5.9×10^{-8} RIU - representing a 340-fold improvement over conventional SPR systems (2.0×10^{-5} RIU). Further signal enhancement was engineered through FDTD-optimized GNR generating localized surface plasmons. This nanostructuring enabled ultrasensitive detection of 17 β-estradiol (LOD: 0.004 ng/mL), demonstrating 180 times greater sensitivity than AuNR-free configurations. The biosensor's modular design shows significant potential for high-throughput screening of endocrine disruptors (e.g., via androgen/thyroid receptors), accelerating global environmental toxicant assessment.

Programmed cell death ligand-1 positive ($PD\text{-}L1^{+}$) exosomes represent clinically significant biomarkers for cancer diagnostics, yet their detection remains challenging due to biological sample complexity, exosomal

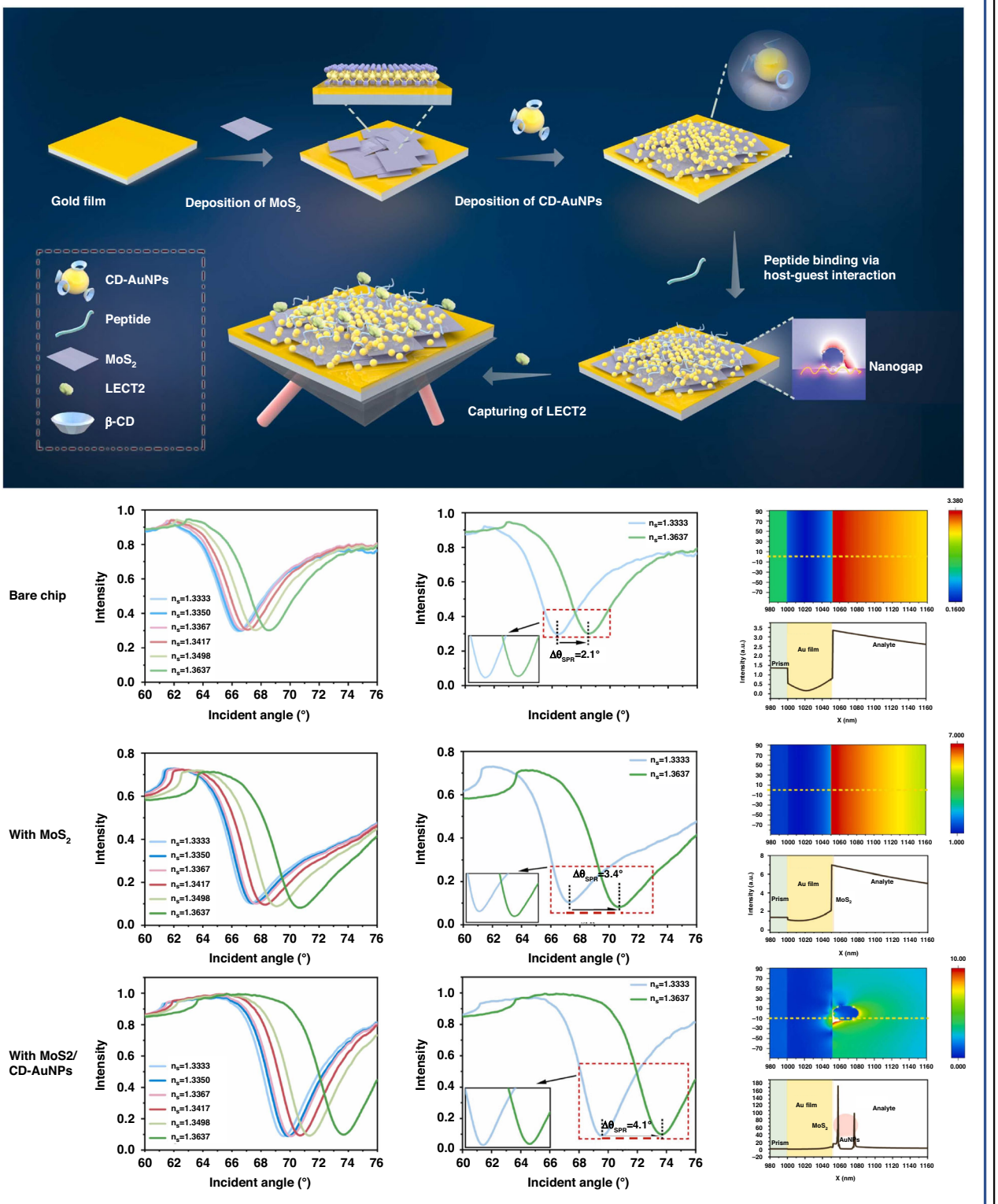

Fig. 7 The principle and results of SPR sensor used for detecting LECT2[205]. Copyright 2024 Elsevier B.V

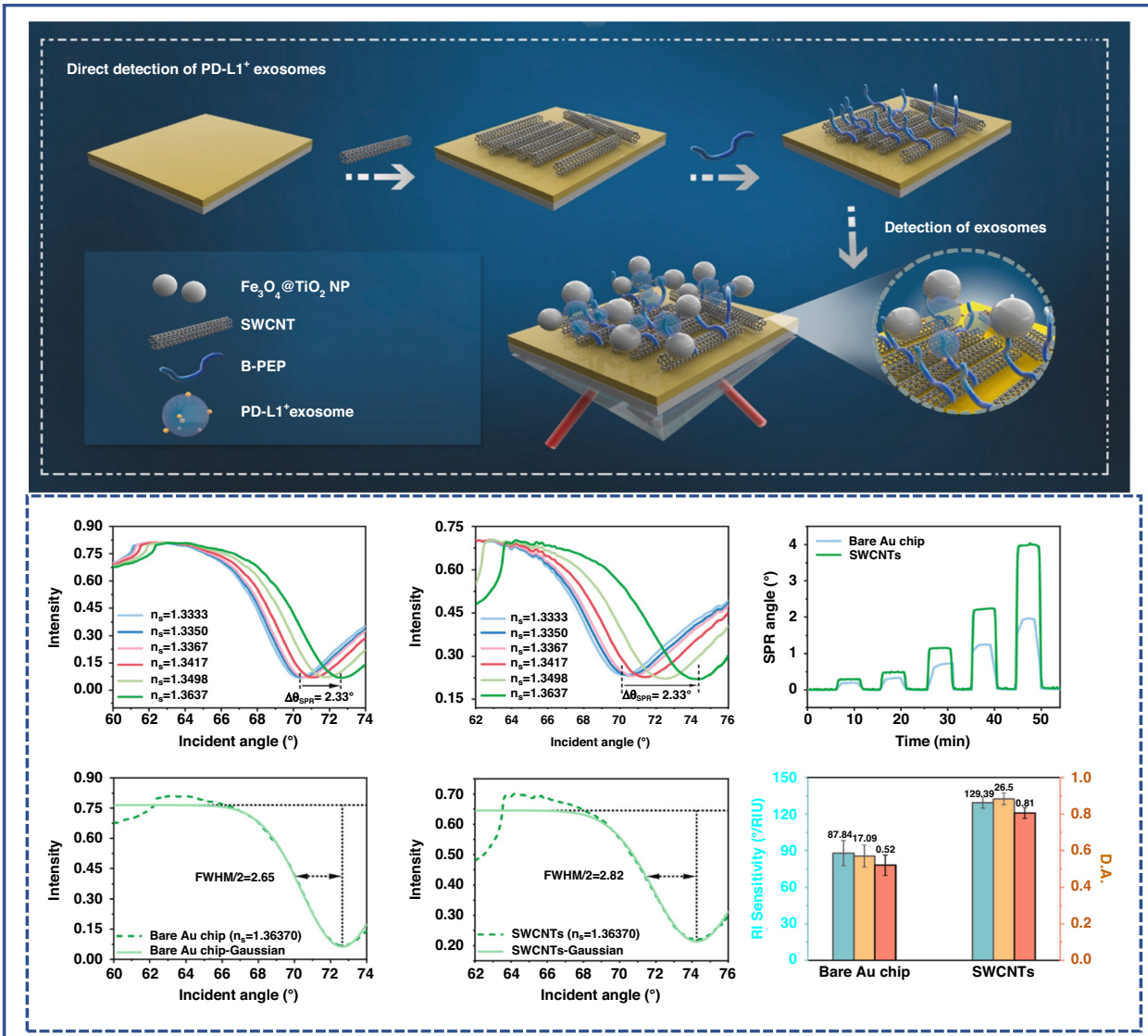

Fig. 8 Diagrammatic illustration of the synthesis process for Fe_3O_4@TiO_2 and the SWCNT-enhanced SPR sensor for detecting the PD-L1$^+$ exosomes[207]. Copyright 2024 Elsevier B.V

heterogeneity, low RI, and inadequate surface coverage on conventional SPR sensors. Liu et al. leveraged the distinctive electro-optical attributes of single-walled carbon nanotubes (SWCNTs) as the substrate material designed an SPR sensor (as shown in Fig. 8)[207], leveraging their exceptional optoelectronic properties and SP^2-hybridized surfaces for biorecognition element immobilization. The platform integrates a magnetic enrichment strategy: Ti^{4+}-phosphate coordination and Fe_3O_4 paramagnetism enable efficient exosome isolation from complex matrices under external magnetic fields. Signal amplification is achieved through high-refractive-index Fe_3O_4@TiO_2 core-shell nanoparticles, significantly enhancing SPR response. This optimized biosensor demonstrates a linear dynamic range of 10^3-10^7 particles/mL with 31.9 particles/mL detection limit. Clinical validation using serum samples achieved near-perfect discrimination (AUC = 0.9835) between cancer patients and healthy controls, establishing a robust platform for direct exosome detection with broad applicability to other low-abundance biomarkers.

Plasmonic metal nanoparticles with optimized LSPR properties significantly enhance SPR sensitivity through resonant plasmonic coupling. The optical response in film-coupled nanoparticle systems critically depends on nanogap architecture. Nucleic acid nanostructures are widely used for precise control of nanoscale gaps due to

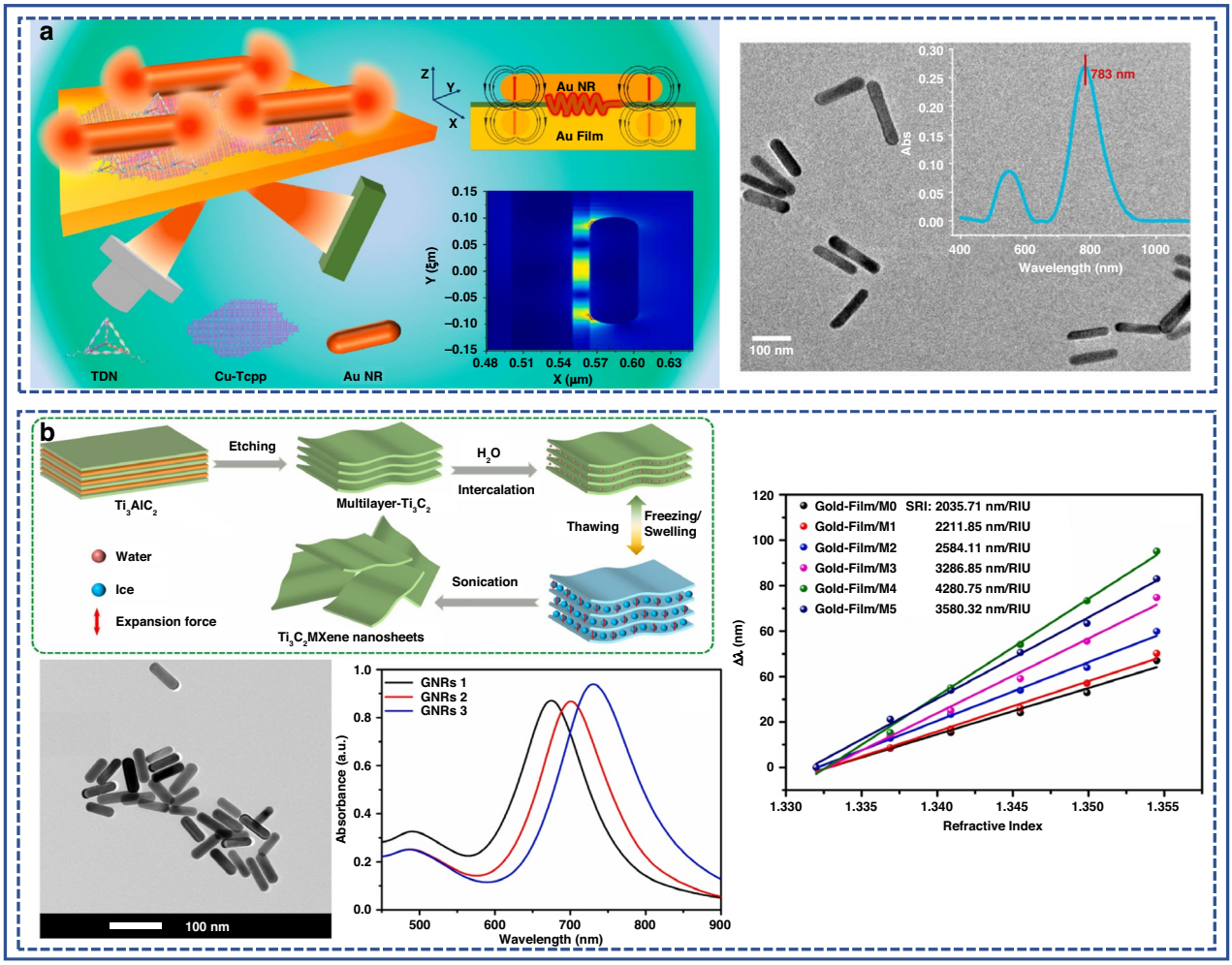

Fig. 9 SPR biosensors based on Metal film and 1D material. a Operational mechanism of the gap plasmon resonance strategy mediated by Cu-TCPP/TDN[208]. Copyright 2023 Elsevier B.V. **b** Diagrammatic illustration of the fabrication of Ti_3C_2 MXene nanosheets using the freeze-thaw and ultrasonic method[209]. Copyright 2025 Elsevier B.V

their excellent stability and flexible structural controllability. 2D metal-organic frameworks (2D MOFs) like Cu-TCPP provide graphene-like conjugated surfaces that enable directional immobilization of nucleic acid assemblies.

Despite these advantages, synergistic integration of nucleic acid nanostructures with 2D MOFs for gap-plasmon systems remains underexplored. Mao et al. constructed a nanoporous scaffold-structured nanogap interposed between a gold film and GNR by integrating the advantages of Cu TCPP assembly membrane and DNA tetrahedral fixation (as shown in Fig. 9a[208]. The DNA tetrahedrons' structural rigidity enables sub-nanometer gap tuning, while their programmable design permits customizable coupling geometries through nucleotide sequence modification. FDTD simulations and experimental validation confirm this design substantially amplifies near-field intensity at the sensor interface, significantly enhancing SPR sensitivity metrics.

1D metal nanorod structures can also be combined with 2D materials to further enhance detection sensitivity through the synergistic effects of plasmonic coupling and charge transfer. Based on this, Zhang et al. proposed a novel optical fiber SPR biosensor with high sensitivity based on Ti_3C_2 MXene/GNR synergy (as shown in Fig. 9b[209]. The sensor probe was functionalized through electrostatic layer-by-layer deposition of Ti_3C_2 MXene and GNRs. This nanostructure configuration yielded a 217% sensitivity enhancement attributed to dual mechanisms: increased evanescent field penetration depth and localized electromagnetic field amplification. For acetylcholine detection, ache was immobilized on polydopamine (PDA)-modified surfaces, achieving a sensitivity of 0.04521 nm/μM with 4.42 μM detection limit. The biosensor demonstrated

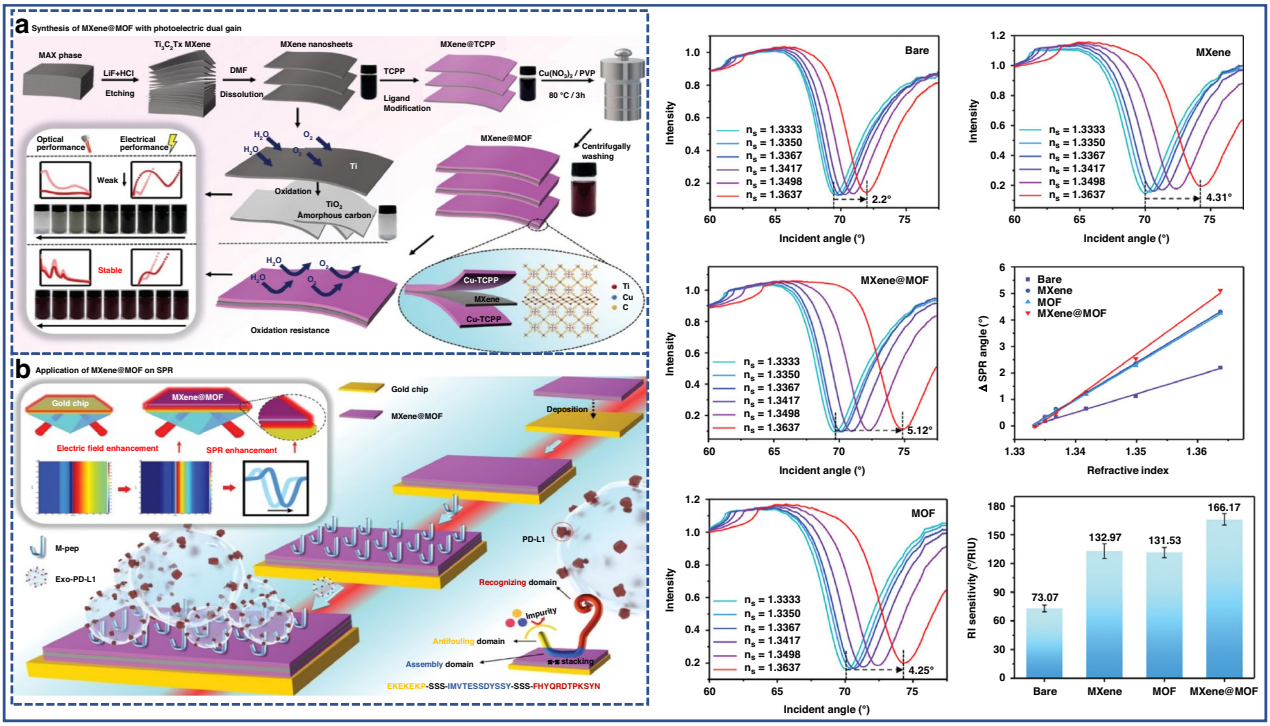

Fig. 10 Demonstration diagram of MXene@MOF-reinforced SPR sensor. a Synthesis process of MXene@MOF, **b** Fabrication procedure of the MXene@MOF-reinforced SPR sensor[214]. Copyright 2023 Wiley-VCH GmbH

96–106% recovery in complex matrices and 220-s response time. This platform shows significant potential for rapid clinical neurotransmitter monitoring with high accuracy.

1D materials, such as GNR, have two plasmon resonance modes (transverse and longitudinal). Its longitudinal mode is coupled with thin film SPP, which can generate strong electromagnetic field enhancement and unique plasma waveguide effect. Seed mediated growth method is the mainstream method for synthesizing GNR, which can precisely control the aspect ratio by adjusting the ratio of seeds to growth solution. In addition, other materials such as nanowires can also be prepared by template method or electrochemical deposition. Similar to 0D nanomaterials, it mainly relies on interface self-assembly, with the key challenge being orientation control. The ideal state is for nanorods to be oriented vertically or parallel to the substrate, but this requires more complex techniques such as external field induction and Langmuir Blodgett membrane technology. By changing the aspect ratio, the LSPR peak can be precisely tuned to a specific wavelength. The "tip effect" of nanorods and their coupling with thin films can generate stronger localized fields than spherical particles. However, the synthesis of nanorods and subsequent orientation control techniques are more difficult and costly than spherical particles. Therefore, the SPR biosensor with metal nanofilm/1D nanomaterial composite structure has a special application position in the research direction of sensors sensitive to the orientation of biomolecules.

Metal film and 2D material

In recent years, 2D materials (such as graphene, transition metal sulfide, MXene, etc.) have been introduced into the design of SPR sensor due to their atomic thickness, high carrier mobility and adjustable electronic characteristics, and the sensing performance has been significantly improved through the synergistic effect with metal film[210–213].

In recent years, the novel 2D material MXene has garnered widespread attention due to its flexible and tunable optoelectronic properties. Despite MXene's exceptional optoelectronic properties enabling widespread use in photonic interfaces, its practical deployment is constrained by ambient oxidation stemming from inherent hydrophilicity and metastability. To address this limitation, Wang et al. engineered a conformal 2D metal-organic framework (MOF) heterojunction on MXene nanosheets[214]. The resulting MXene@MOF heterostructure demonstrates ideal characteristics for SPR sensitization layers (as shown in Fig. 10). Experimental and computational analyses (FDTD simulations, DFT calculations) reveal its signal amplification mechanism involves:

plasmonic near-field enhancement and charge transfer optimization at the hybrid interface. Leveraging these properties, an MXene@MOF/peptide-functionalized SPR biosensor achieved rapid, ultrasensitive detection of exosomal cancer biomarkers. This work establishes a generalized design principle for creating oxidation-resistant photonic materials with tailored interfacial properties.

Ultrasensitive exosome detection is critical for early disease diagnostics and monitoring. Jia et al. proposed a label free SPR aptamer sensor based on 2D ultra-thin cobalt borate nanosheets embedded with aptamer template silver nanoclusters (APT/AgNCs@-CoB)[215]. By utilizing the plasmonic coupling mechanism between AgNCs and the Au film, as well as the charge transfer mechanism between cobalt borate nanosheets and the Au film. It is used for sensitive detection of exosome marker CD63 (as shown in Fig. 11). The APT/AgNCs@CoB Schottky junction enhances plasmonic coupling through high absorption synergizing with SPR evanescent fields and localized surface plasmons from AgNCs boosting interfacial electron transfer and embedded aptamers ensuring stable probe anchoring and target affinity. This nanoarchitecture enables single-step gold chip functionalization, significantly enhancing sensitivity for direct CD63 quantification. The biosensor achieved a low LOD: 0.15 fg/mL. This APT/AgNCs@CoB-based platform establishes a novel sensing paradigm for exosome marker detection with transformative potential in non-invasive cancer diagnostics.

Improving the sensitivity of SPR sensor is a crucial research field, because it can detect the interaction between low concentrations of analytes and small biomolecules. By combining GO with plasmon silver film polydimethylsiloxane (PDMS) hybrid nanostructures, Zhao et al. developed a biosensor with excellent sensitivity and FOM (as shown in Fig. 12)[216]. The GO-functionalized platform exhibited an average RI sensitivity 33.6 μm/RIU, a 20.5% enhancement compared with the baseline Fano resonance sensor (27.9 μm/RIU). And the FOM rose by 36.3% to 2383.82 RIU^{-1}. Validated through carcinoembryonic antigen (CEA) detection, the biosensor exhibited a sensitivity of 5.2 nm/(ng/mL), a detection limit 63.5 pg/mL and good selectivity. This performance advancement positions technology as a promising platform for early cancer diagnostics and high-resolution biomolecular interaction studies.

Recently, Zhu et al. developed a GHS SPR biosensor based on $Ge_2Sb_2Te_5$ (GST) thin film (as shown in Fig. 13)[63]. The GST layer not only enhances the GH shift, but also prevent oxidation of the silver film. This biosensor obtained a 439.3 μm GHS and a 1.72×10^8 nm RIU^{-1} detection sensitivity. Additionally, the detection limit is 6.97×10^{-7} RIU, with a positional resolution of 0.12 μm and a large FOM of 4.54×10^{11} μm RIU^{-1}.

The metal film and 2D material composite structure promotes the detection limit of SPR sensor to single molecule or fg/mL level through charge transfer, exciton coupling, mechanical adaptation and other mechanisms, and extends to wearable, multi-target detection and other scenarios. In the future, with the expansion of 2D material library (such as Janus materials, antiferromagnetic materials) and the progress of micro nano processing technology, this field is expected to achieve greater breakthroughs in precision medicine, environmental monitoring and other fields.

2D materials enhance the detection sensitivity of SPR sensors through physical adsorption, charge transfer, and exciton-plasmon coupling. The key to SPR biosensors based on 2D materials lies in controlling the number of layers of 2D materials, reducing defects and pollutants. The material prepared by liquid-phase exfoliation method has uneven layers and many defects, which affect the consistency of performance. The CVD combined with wet transfer process is lengthy and the yield needs to be improved. 2D materials have broad prospects in quantitative detection due to their regular surface structure. The combination of metal nanofilm and 2D materials composite structure is a very promising solution for large-scale clinical translation.

Metal film and metasurface structure

Metasurface is a 2D artificial material composed of subwavelength structure. It has been introduced into the design of SPR sensor because of its ability to accurately control the wavefront, phase and polarization of light[217]. By combining the super surface with the metal film, researchers can break through the physical limitations of the traditional structure and realize the comprehensive improvement of sensitivity, selectivity and versatility.

The metal film and metasurface composite structure can advance the detection limit of SPR sensor to fg/mL or even single molecule level through vortex light field, Fano resonance, chiral regulation and other mechanisms, and expand to new scenarios such as wearability and enantiomer recognition. In the future, with the development of super surface design tools (such as deep learning reverse design) and advanced manufacturing technology, this field is expected to achieve greater breakthroughs in precision medicine, personalized health monitoring and other fields.

The plasmon metasurface (PM) exhibits extraordinary optical response due to surface lattice resonance, which is very important for the preparation of high-performance photovoltaic devices. In the work of Wang et al., based on nanopore confinement effect mediates MOF@UsAu, a novel PM heterojunction for photovoltaic interface is proposed (as shown in Fig. 14)[218]. 2D MOF enable precise plasmonic engineering through their structurally

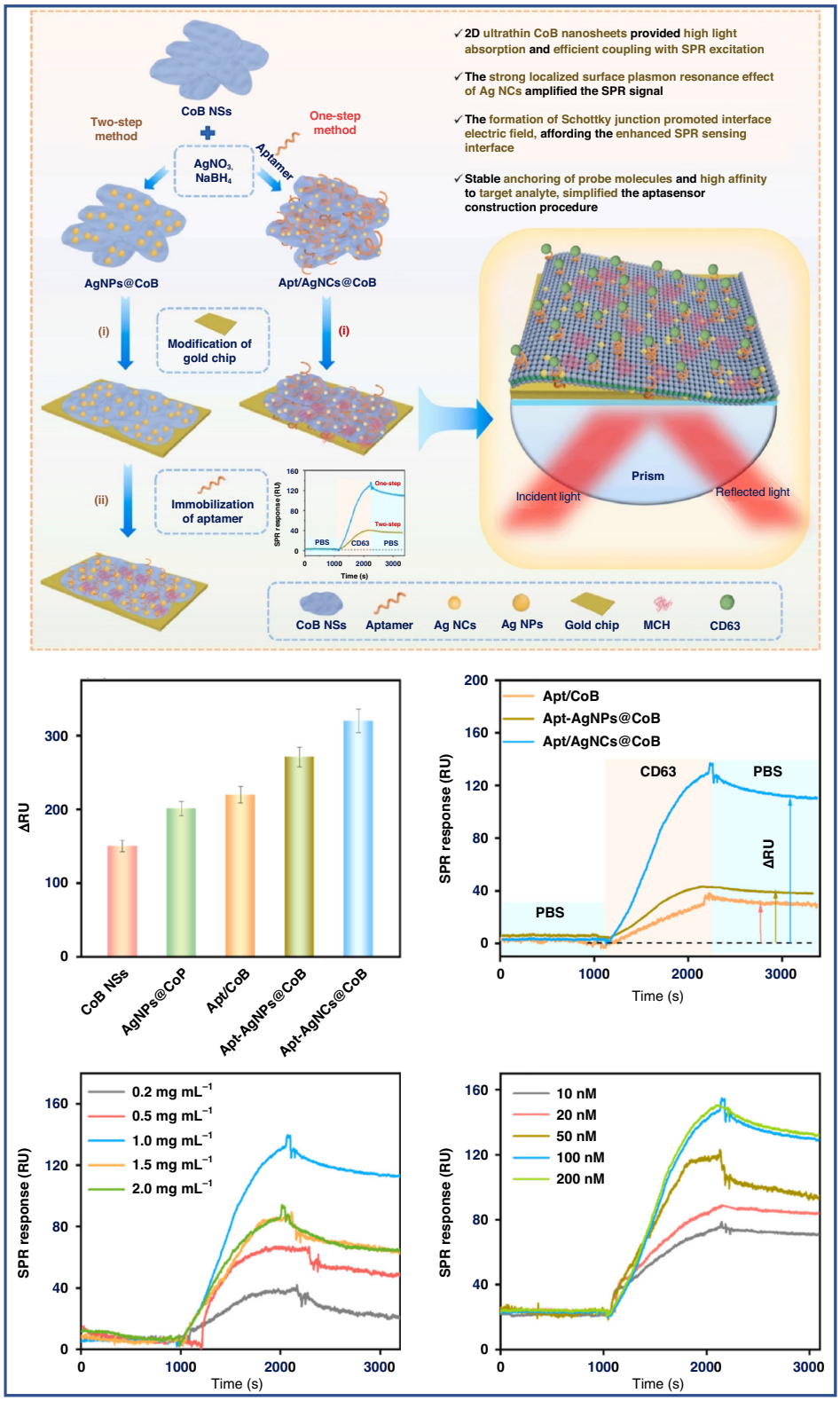

Fig. 11 Diagrammatic scheme of the SPR aptasensor for exosomal CD63 detection utilizing the Apt/AgNCs@CoB hybrid as the sensing layer[215]. Copyright 2025 Elsevier B.V

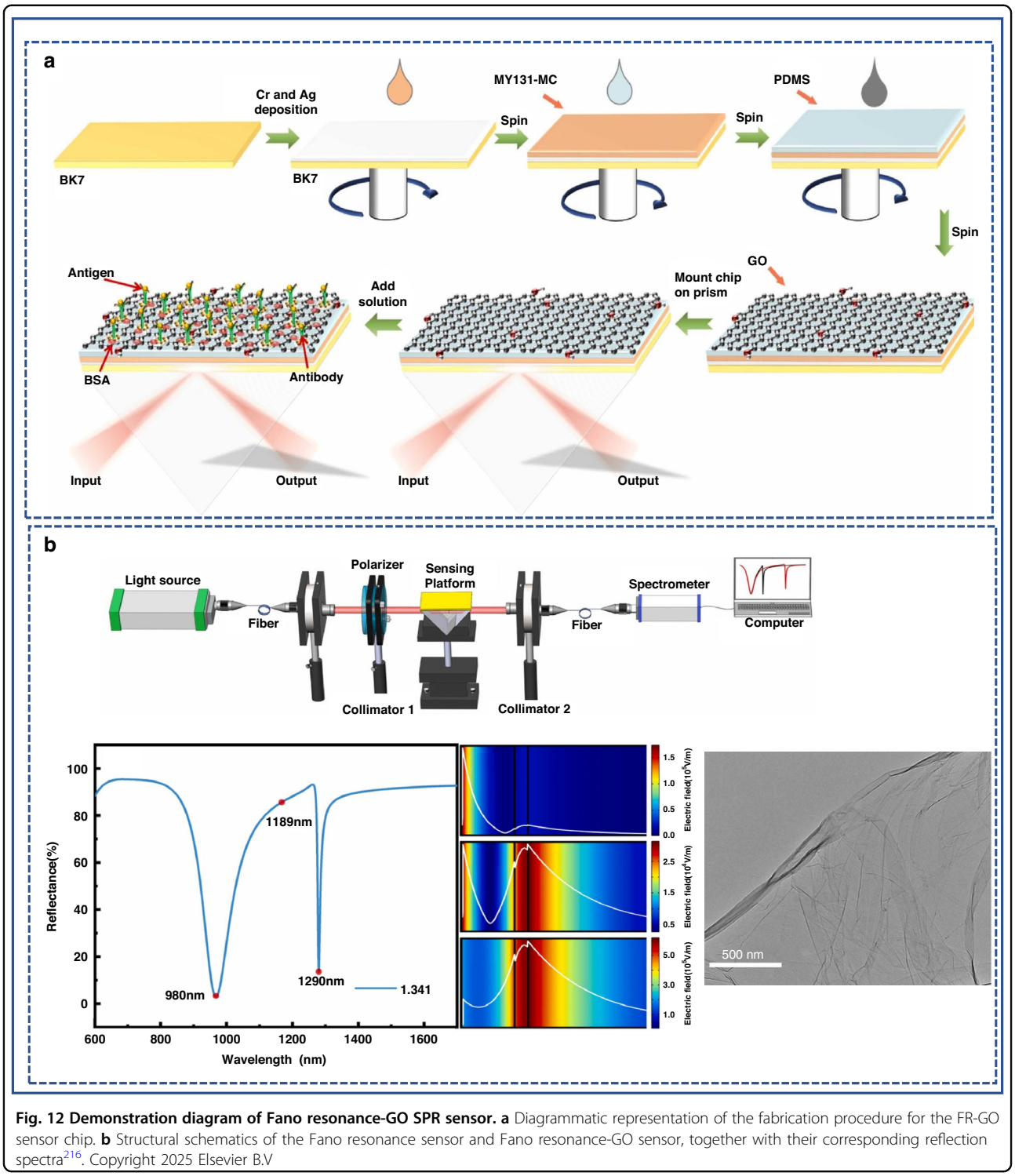

Fig. 12 Demonstration diagram of Fano resonance-GO SPR sensor. a Diagrammatic representation of the fabrication procedure for the FR-GO sensor chip. **b** Structural schematics of the Fano resonance sensor and Fano resonance-GO sensor, together with their corresponding reflection spectra[216]. Copyright 2025 Elsevier B.V

ordered nanopores. This architecture regulates in situ synthesis of AuNPs on MOF surfaces with controlled size and spatial distribution. The heterojunction exhibits enhanced plasmonic-photovoltaic (PM) responses due to interface delocalization from work function matching, schottky barrier formation via band bending and localized SPR amplification at the plasmonic-semiconductor interface. These effects collectively intensify the SPR evanescent field. Leveraging this platform, a PM-enhanced SPR biosensor functionalized with S-shaped bifunctional peptides was constructed for detection of tumor exosomes. The strategy establishes a

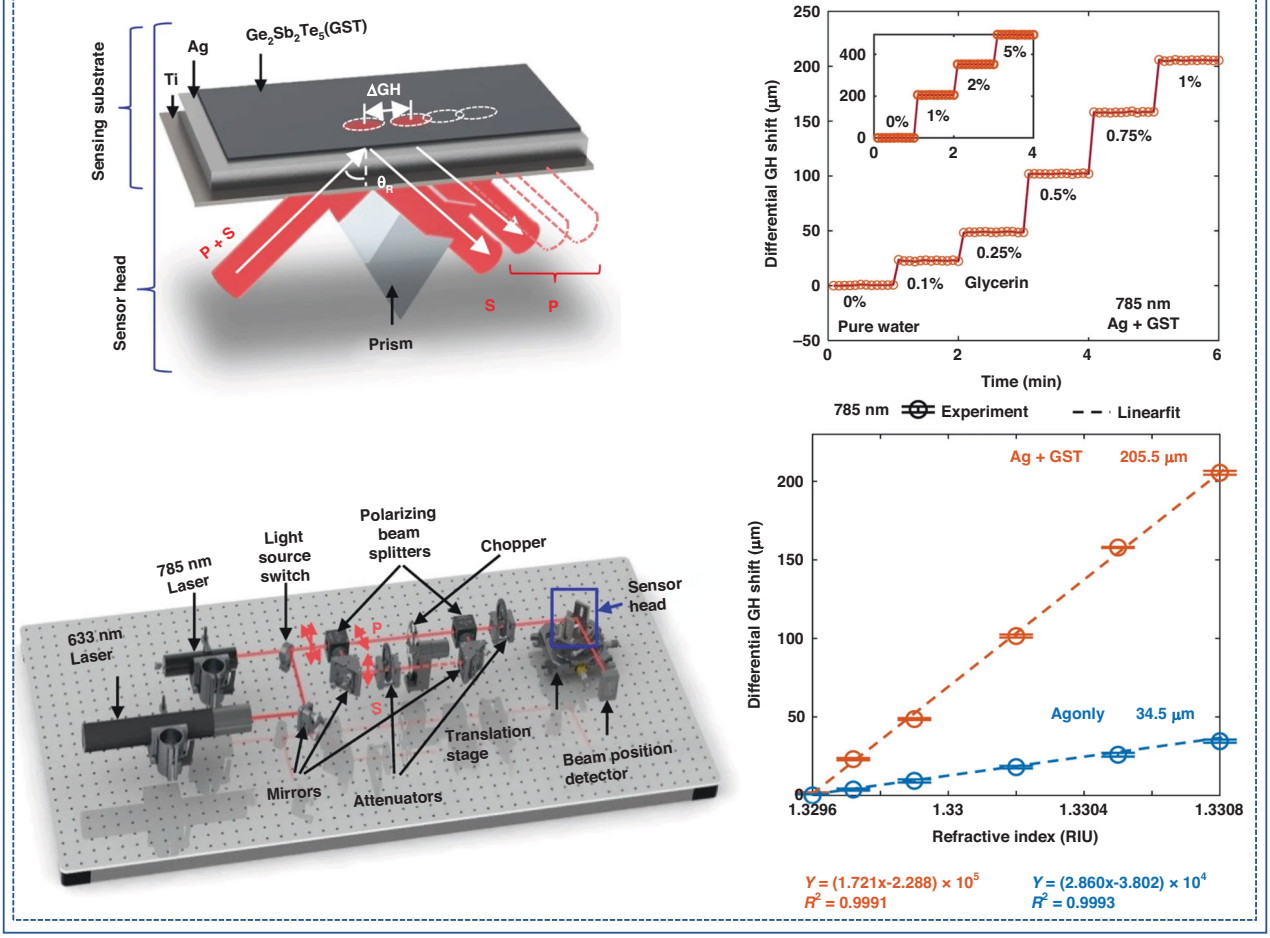

Fig. 13 Singular phase enhanced plasmonic sensor[63]. Copyright 2025 Springer Nature Limited

novel paradigm for designing advanced plasmonic materials and tailored optoelectronic interfaces, with potential applications across photovoltaic devices and biosensing platforms.

Considering that it is very desirable to improve the detection of biological analytes for affinity analysis, Chen et al. established an imaging system based on metasurface plasmon resonance (meta SPR)[219], which integrates the LSPR sensing platform with diverse microfluidic systems and employs straightforward bright-field imaging (as shown in Fig. 15). The system is capable of conducting low-level analyte concentration analysis within the range of 100 pM to 100 nM, and remove non-specific binding signals in real time in the field of vision of the same equipment. Combined with microfluidic system and micro drop sample, the kinetic curves of samples under ten concentration gradients can be automatically measured, or the specific reactions of multiple samples can be detected simultaneously in a single experiment. The system can realize complex detection functions cheaply and conveniently, showing the innovative breakthrough of sensor detection.

SPR sensing technology has the advantages of label free, high sensitivity, and rapid accuracy, and has important application value in clinical diagnosis. In response to the issues of insufficient sensitivity and low selectivity encountered in the detection of trace exosomes in complex serum, Zhou et al. developed a core-shell structured Au@SiO_2−gold film[220]. This work establishes a tunable gap-mode plasmonic architecture to amplify SPR signals through engineered Au@SiO_2 nanoparticle metasurfaces. Precise gap manipulation creates 3D-enhanced evanescent fields via in-plane/out-of-plane coupled Au@SiO_2 NPs, spatially matching exosome dimensions (50–150 nm). Self-assembled bifunctional peptides provide simultaneous recognition ($PD\text{-}L1^+$ exosomes) and antifouling capabilities. They attained a high sensitivity (0.16 particles/mL) and a broad response range ($10–5 \times 10^3$ particles/mL) by optimizing the SiO_2 thickness and surface coverage of

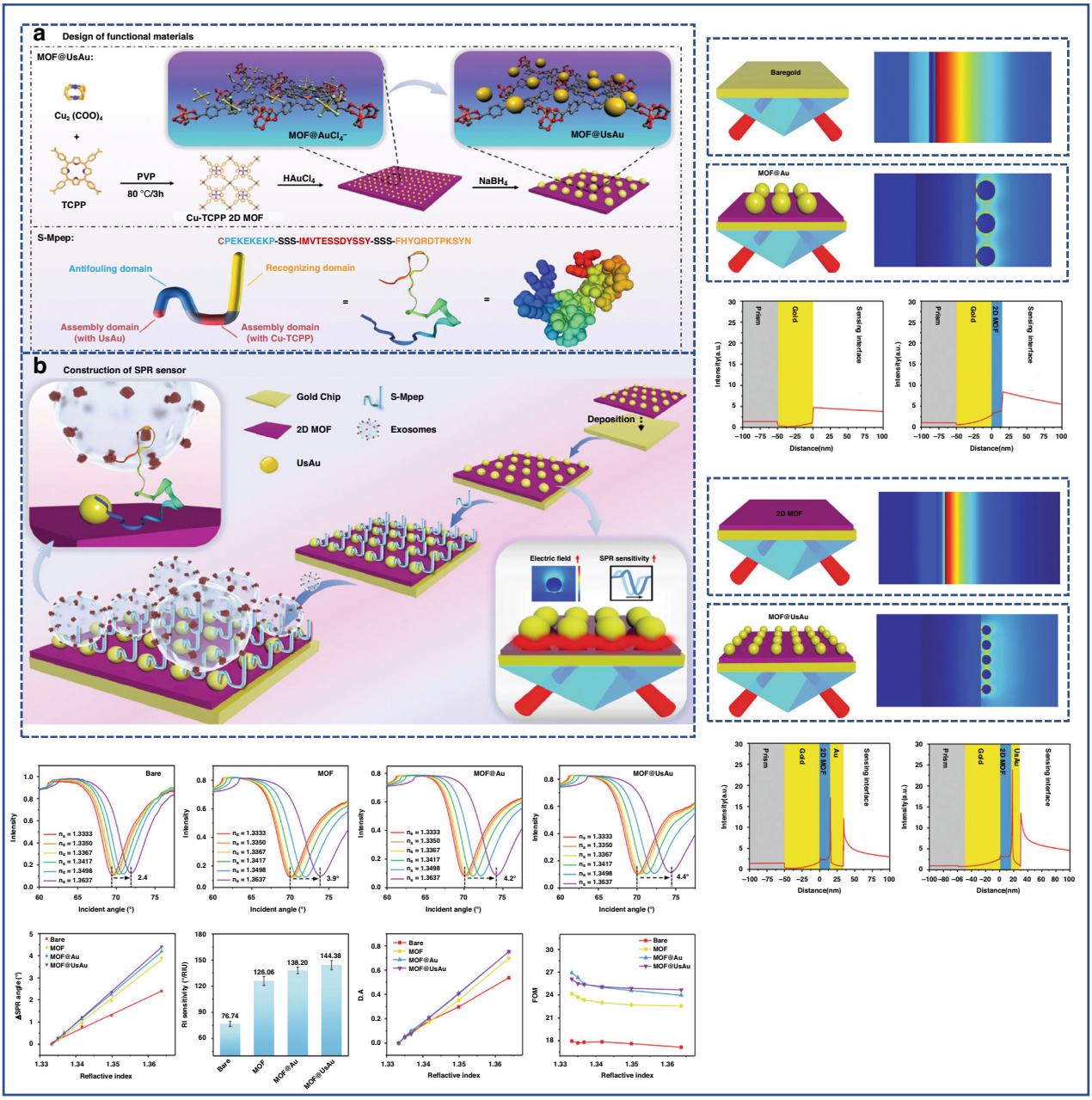

Fig. 14 Schematic diagram of PM-enhanced SPR sensor. a the design and synthesis of MOF@UsAu and S-Mpep. **b** the development process of PM-enhanced SPR sensor for exosomes[218]. Copyright 2024 Wiley-VCH GmbH

$Au@SiO_2$. Clinically validated with serum samples, the biosensor achieved exceptional diagnosis accuracy (AUC = 0.97) discriminating clinical patients from healthy individuals. The systematic study on the relationship between gap mode and SPR sensitivity provides a broad range for promoting the direct, efficient, high selectivity of SPR sensor in clinical application.

Recently, Liu et al. designed a differential guided mode resonant SPR sensor with thickness modulation reaching tens of nanometers, achieving a significant improvement in sensitivity and reducing the trade-off of sensitivity dynamic range(as depicted in Fig. 16)[23]. It can be found that, the sensitivity of each RIU can reach up to 1 million pixels, which is nearly three orders of magnitude higher than existing technologies, and the incident angle has been reconfigured with a larger dynamic range. This design achieves FOM of 10^4 RIU^{-1}. It indicates that, this sensor has the potential to be

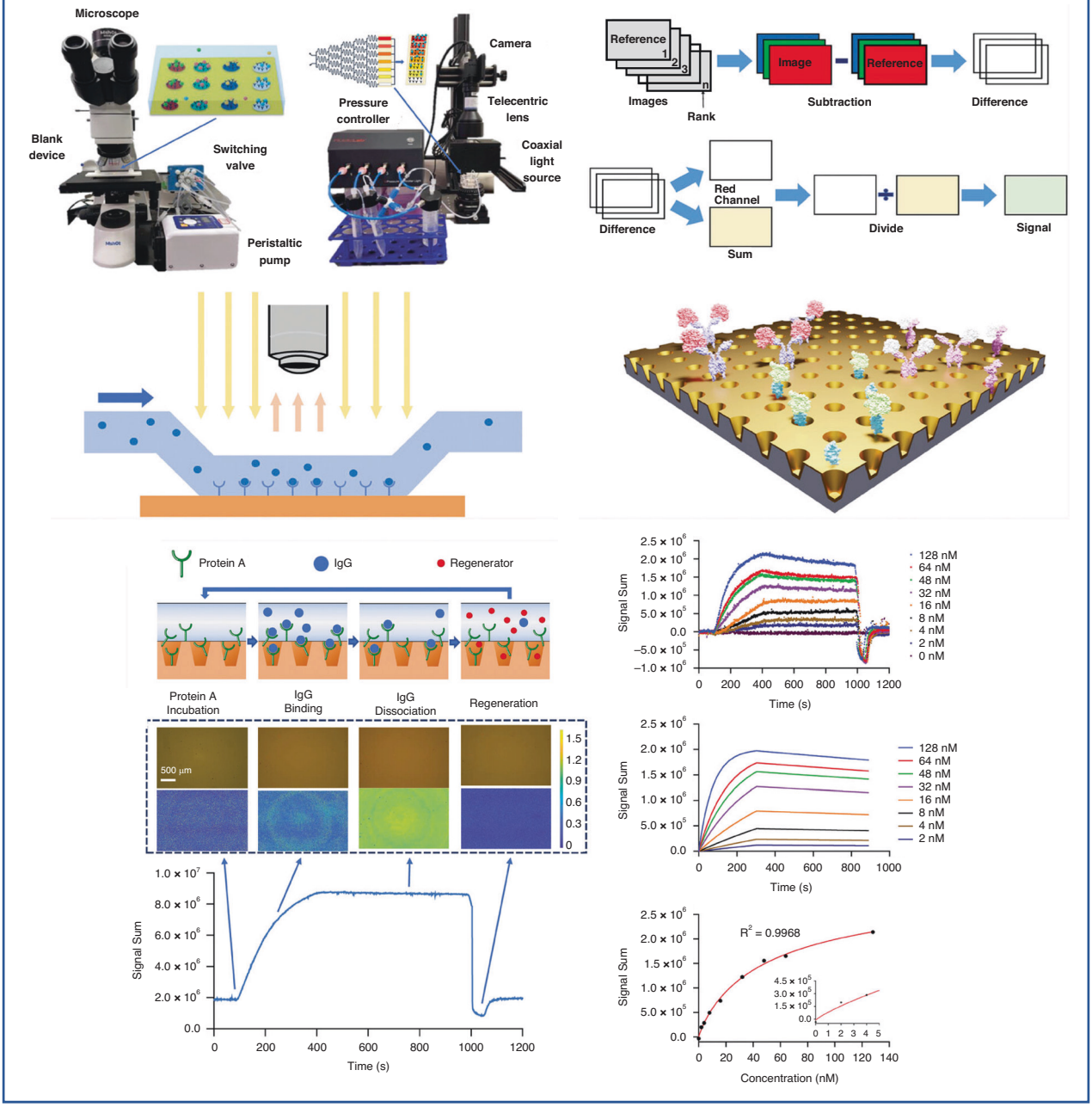

Fig. 15 Scheme of the imaging-based Meta-SPR affinity analysis system[219] Copyright 2024 Wiley-VCH GmbH

applied in biochemical analysis and precision medical testing field.

Another work of Lee et al. introduced a plasmonic sensor utilizing a quantum tunnel junction as an embedded light source(as shown in Fig. 17)[221]. The top contact of the junction adopts an optical resonant dual period nanowire metasurface, which provides uniform emission at a larger size and amplifies the mode through a plasma nanoantenna, thereby obtaining enhanced spectral and RI detection sensitivity. As a proof of concept, spatially resolved RI sensing of nanometer-thick polymer and biomolecule coatings was demonstrated. The authors believe that this research result opens up exciting prospects for integrated electro-optic biosensors based on disruptive platforms.

The metal nanofilm/metasurface composite structure is not simply a “material” composite, but a “structure”

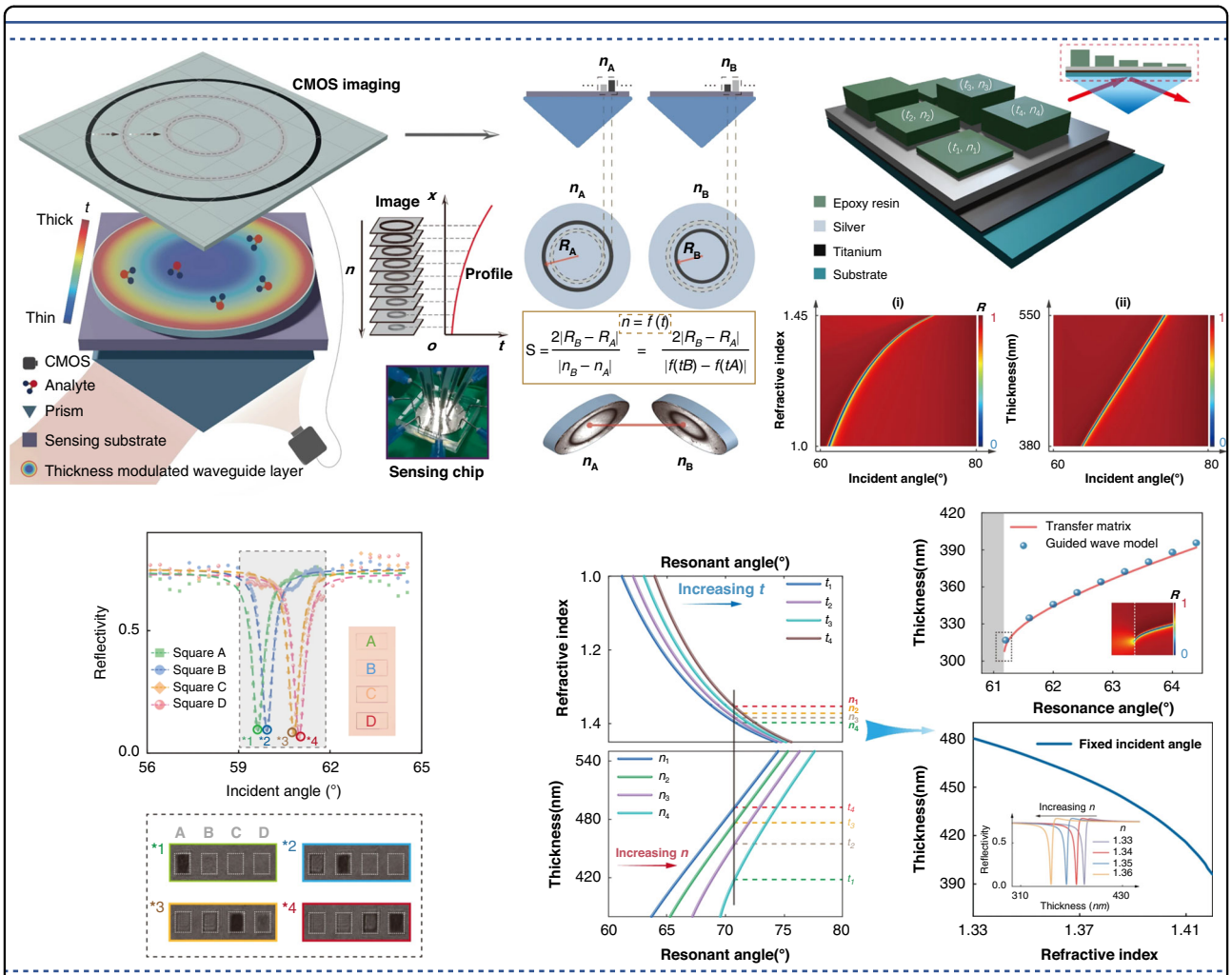

Fig. 16 Diagrammatic sketch of the thickness-modulated SPR imaging sensor[23]. Copyright 2025 Springer Nature Limited

composite. By using techniques such as electron beam lithography, periodic sub wavelength structures (such as nanopore arrays and nanocolumn arrays) are constructed on metal thin films to form metasurfaces. The coupling mechanism involves strong hybridization between SPP and these artificial structural units, such as Fabry-Perot cavity resonance and magnetic resonance, resulting in anomalous optical phenomena such as quasi-BIC and Fano resonance. Therefore, top-down micro nano processing techniques can be fully introduced for the manufacturing of SPR biosensors, including electron beam lithography, focused ion beam etching, and nanoimprint technology. The sharp resonance lines such as Fano resonance are extremely sensitive to changes in the surrounding dielectric environment, and can achieve huge wavelength/angle shifts under small RI unit changes, which can be used for single-molecule detection. The structural parameters (shape, size, period) can be precisely designed to ensure high consistency and reproducibility between sensors. However, this approach generally suffers from extremely high preparation costs, which is the biggest obstacle to its progress towards routine clinical diagnosis. It is more likely to be first applied in cost insensitive ultra-high sensitivity detection fields, such as top-level scientific research, cutting-edge drug development, or specialized testing.

Summary and outlook

The SPR biosensors based on composite nanostructures have significantly improved the sensitivity, selectivity and versatility through the synergistic effect of metal/non-metal nanostructures and plasmonic thin films, so it is considered to be a development direction in the field of SPR biosensors. In recent years, the wide application of nanostructures of various materials has greatly improved the detection sensitivity of SPR biosensors. This Review has summarized the research status of various

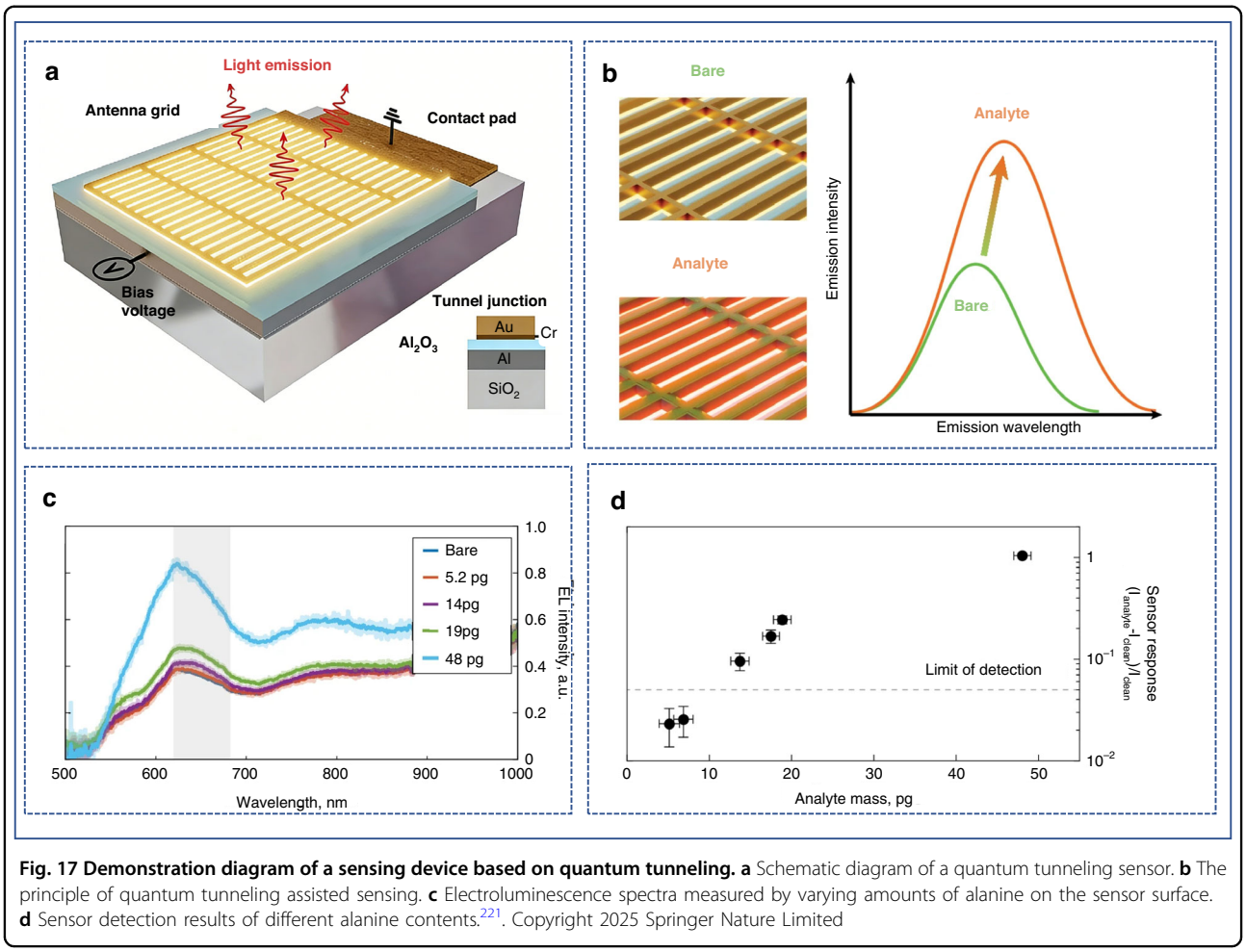

Fig. 17 Demonstration diagram of a sensing device based on quantum tunneling. a Schematic diagram of a quantum tunneling sensor. **b** The principle of quantum tunneling assisted sensing. **c** Electroluminescence spectra measured by varying amounts of alanine on the sensor surface. **d** Sensor detection results of different alanine contents.[221]. Copyright 2025 Springer Nature Limited

nanoparticles employed in SPR biosensors to improve the detection sensitivity in recent years, elaborated the theoretical explanations of different nanostructures to enhance the sensitivity, introduced the preparation methods of nanostructures, and illustrated the important progress in the direction of nanostructures to improve the detection sensitivity of SPR biosensors. We infer that the observed findings presented herein indicate that diverse nanostructurs-enhaced SPR biosensing platforms are capable of significantly outperforming conventional SPR substrates, attributed to their ultrahigh detection sensitivity, as summarized in Table 1.

At present, three main types of nanostructures, including nanoparticles, 2D materials and metasurface structures, are widely used in the design and development of SPR biosensors. Based on this, SPR biosensors are widely used in disease diagnosis, virus detection, water quality detection and many other fields. Although nanostructures are important in the designing and developing SPR biosensors, the development prospects still face the following key challenges:

1. The performance of nanostructures is highly dependent on the size, morphology and spatial arrangement accuracy of nanounits (such as nanoparticle spacing, metasurface period, etc.). The existing preparation technologies (such as chemical synthesis method, CVD method, etc.) also present the problems of low accuracy and low efficiency in the accurate preparation of nanostructures.
2. Metal nanostructures (such as silver and copper) are prone to oxidation or vulcanization, leading to SPR signal drift; Nonspecific adsorption (such as protein and cell debris) in biological samples will cover the active sites and reduce the reliability of detection. Flexible sensors are prone to structural fatigue or interface peeling under mechanical deformation.
3. Although FDTD, DDA and other simulation tools can accurately predict the field enhancement effect of composite structures, the experimental sensitivity is often lower than the theoretical value due to interface defects, material loss and other factors in actual devices. The main reason is that the surface roughness of materials, the size distribution of

Table 1 Comparison of various nanostructurs-enhaced SPR biosensing platforms. (Selected)

Biosensing platform	Preparation Method	Sensitivity enhancement mechanism	Signal modulation	Target analytes	Sensitivity/LOD	Ref.
Au/AuNPs	liquid phase method	SPR-LSPR coupling	phase modulation	pathogenic H9N2 viruses	(1.04×10^{-5} fM)	201
Au/AuNPs	liquid phase method	SPR-LSPR coupling	angle modulation	cortisol	104.687 deg/RIU	222
Au/AuNPs/(MXene-TA-Au-PEG)	physical mechanical exfoliation + self-assembled + liquid phase method	SPR-LSPR coupling+ charge transfer	angle modulation	exosome	176.20 deg/RIU	203
Au/AuNPs	liquid phase method	SPR-LSPR coupling	intensity modulation	miRNAs	0.57 pM and 0.83 pM for miR-183 and miR-155	204
Au/MoS_2/AuNPs	liquid phase method	SPR-LSPR coupling	angle modulation	LECT2	133.3 deg/RIU	205
Au/AuNRs	liquid phase method	SPR-LSPR coupling	feedback light-induced intensity modulations	endocrine-disrupting chemicals	5.9×10^{-8} RIU	206
Au/single-walled carbon nanotubes/ Fe_3O_4@TiO_2,	arc plasma jet approach + liquid phase method	SPR-LSPR coupling	angle modulation	$PD\text{-}L1^+$	129.39 deg/RIU	207
Au/2D MOF(Cu-TCPP)-AuNRs	liquid phase method	SPR-LSPR coupling	angle modulation	$PD\text{-}L1^+$	253.31 deg/RIU	208
Au/Ti_3C_2 MXene/GNRs	liquid phase method + self-assembly	SPR-LSPR coupling	wavelength modulation	acetylcholine	0.04521 nm/μM	209
Ag/$Ge_2Sb_2Te_5$ (GST)	magnetron sputtering	charge transfer	GH shift modulation	small biological molecules/ cancer markers	1.72×10^8 nm /RIU	63
Au/Mxene@MOF	liquid phase method	charge transfer	angle modulation	$PD\text{-}L1^+$	166.17 deg/RIU	214
Au/Apt/AgNCs@CoB	liquid phase method	SPR-LSPR coupling+ charge transfer	intensity modulation	exosomal marker CD63	320 a.u LOD: 0.15 fg /mL	215
Ag/GO	liquid phase method	Fano resonance+ charge transfer	wavelength modulation	carcinoembryonic antigen	5.2 nm/(ng/ml)	216
Au/ 3D tuning hypersurface	electron beam evaporation	tune the resonant wavelength	wavelength modulation	D-biotin	100 μm/RIU, 27.5 fM(LOD)	54
Au/Au@SiO_2	liquid phase method + self -assembled	SPR-LSPR coupling	angle modulation	$PD\text{-}L1^+$	0.16 particles/mL	220
Au nanopore array metasurface	laser interference lithography + ion etching	SPR-LSPR coupling	intensity modulation	IgG	0.5–64 nm(LOD)	219
Au/2D MOF@UsAu	liquid phase method + self-assembled	SPR-LSPR coupling + charge transfer	angle modulation	$PD\text{-}L1^+$	144.38 deg/RIU	218

nanoparticles and the fluctuation of ambient temperature and humidity are often ignored in the simulation. The theoretical model of this direction is of great significance for the development of SPR biosensor technology.

In order to overcome the above challenges and meet the future development needs of SPR biosensors based on composite nanostructures, we need to continue to make efforts in the direction of material innovation, device design and system integration:

1. Pay attention to the development of material synthesis, especially the synthesis and preparation of nanomaterials, and develop nanostructures with accurate structure control and reliable performance for the design and development of SPR biosensors by combining new technologies and methods. For example, biomimetic nanoparticles on cell membranes can achieve specific capture and signal amplification by utilizing their high affinity with target cells, such as circulating tumor cells. This nanoparticle preparation scheme is expected to provide new ideas for the development of SPR biosensors. In addition, the synthesis method of molecularly imprinted nanoparticles involves preparing nanomolecularly imprinted polymers as artificial antibodies, providing highly specific binding sites for efficient capture of target molecules. This approach has certain potential for specific detection based on SPR biosensors in the future;
2. Continue to promote the integration of new low dimensional materials and the development of Interface Engineering, develop new low dimensional materials such as MXene, Janus 2D materials and silicon carbide quantum dots, optimize charge transfer and light matter interaction through energy band engineering and interface modification (such as covalent bonding and vdWhs), and enhance SPR signal. The future development trend will focus on multi material collaboration (such as ternary heterostructure design), new 2D materials with flexible and adjustable optoelectronic properties (such as MXene), and functional modified 2D materials for practical applications. MXene is considered the most promising 2D material in the field of SPR biosensors due to its extremely high conductivity and rich surface chemical functional groups, making it easy to modify. Moreover, when combined with gold film, it can generate strong electromagnetic field enhancement;
3. Real time regulation of SPR resonance wavelength, sensitivity and detection mode is realized by combining with new materials such as integrated phase change materials, liquid crystals or stimulus responsive hydrogels. To date, various new nanomaterials with adjustable features have been prepared through nanomaterial defect engineering, providing new research ideas for the development of SPR biosensors. By providing highly active sites through atomic level defect engineering, in situ growth of AuNPs is achieved, achieving strong coupling between LSPR and SPR. In addition, the novel nanomolecularly imprinted polymer can serve as an artificial antibody, providing high affinity binding sites;
4. Use deep learning to optimize the design of composite nanostructures, and develop intelligent algorithms to analyze complex biological signals. The optimal nanostructure parameters are predicted by generating an adversary network. Traditional SPR data analysis is primarily based on preset models, and its ability to analyze complex systems is limited. However, machine learning algorithms can automatically and efficiently extract high-dimensional features from complex and noisy spectral or kinetic data, identifying subtle relationships that are unrecognizable by the human eye or traditional methods.

Firstly, as the "brain", machine learning algorithms can be integrated with sensor control systems to enable real-time decision-making. During data acquisition, they can assess data quality in real time, automatically flag issues or abort invalid experiments, thereby saving time and reagents. Based on the characteristics of real-time binding curves, they can automatically adjust measurement parameters to optimally capture key kinetic information. They can automatically identify the type of binding event and directly provide preliminary conclusions or classification results, reducing the reliance on the operator's professional experience. By precisely analyzing overlapping resonance peaks, they enable simultaneous, label-free detection and quantitative analysis of multi-component mixtures. Secondly, by recognizing the unique "spectral fingerprints" brought by different molecular binding events, they can effectively distinguish between specific and non-specific binding, significantly reducing false positive signals. Most importantly, by using ML algorithms, they can more robustly and automatically calculate binding kinetic constants, enabling the analysis of weak or rapid binding processes.

In the foreseeable future, through supervised learning and generative models, machine learning can learn the complex mapping relationship between SPR response and various interferences. By effectively filtering out background noise and improving SNR, the LOD can be indirectly reduced, making it possible to detect biomarkers at extremely low concentrations.

SPR biosensors based on composite nanostructures are at a critical stage from laboratory innovation to industrial application. Despite the challenges of preparation, stability and standardization, through the integration of new materials, dynamic control, multimodal integration, artificial intelligence and other cutting-edge technologies, its detection limit is expected to further approach the single molecule level, and expand to new scenarios such as wearable medicine and in vivo monitoring. In the future, the deep integration of interdisciplinary collaboration (materials science, optical engineering, biomedicine) and industry university research will become the core driving force to promote breakthroughs in this field, and ultimately realize the large-scale application of SPR technology in precision medicine and personalized health management.

Acknowledgements
This work was partially supported by the National Key Research and Development Program of China "National Quality Infrastructure" (Grant No. 2021YFF0600902), the National Natural Science Foundation of China (62075137), the Guangdong Basic and Applied Basic Research Foundation (2023A1515140161), the Dongguan Science and Technology of Social Development Program (20231800936312), and the high-level talent program of Dongguan University of Technology (No. 221110080).

Conflict of interest
The authors declare no competing interests.

Received: 30 July 2025 Revised: 10 October 2025 Accepted: 30 October 2025
Published online: 28 January 2026

References

1. Brolo, A. G. Plasmonics for future biosensors. *Nat. Photonics* **6**, 709–713 (2012).
2. Nguyen, H. H., Park, J., Kang, S. & Kim, M. Surface plasmon resonance: a versatile technique for biosensor applications. *Sensors* **15**, 10481–10510 (2015).
3. Wang, Q. et al. Research advances on surface plasmon resonance biosensors. *Nanoscale* **14**, 564–591 (2022).
4. Shrivastav, A. M., Cvelbar, U. & Abdulhalim, I. A comprehensive review on plasmonic-based biosensors used in viral diagnostics. *Commun. Biol.* **4**, 70 (2021).
5. Wang, Y., Plummer, E. W. & Kempa, K. Foundations of plasmonics. *Adv. Phys.* **60**, 799–898 (2011).
6. Pitarke, J. M., Silkin, V. M., Chulkov, E. V. & Echenique, P. M. Theory of surface plasmons and surface-plasmon polaritons. *Rep. Prog. Phys.* **70**, 1 (2007).
7. Yesudasu, V., Pradhan, H. S. & Pandya, R. J. Recent progress in surface plasmon resonance based sensors: a comprehensive review. *Heliyon* **7**, e06321 (2021).
8. Springer, T. et al. Surface plasmon resonance biosensors and their medical applications. *Biosens. Bioelectron.* **278**, 117308 (2025).
9. Li, L. et al. Dielectric surface-based biosensors for enhanced detection of biomolecular interactions: advances and applications. *Biosensors* **14**, https://doi.org/10.3390/bios14110524 (2024).
10. Chen, T., Xin, J., Chang, S. J., Chen, C. J. & Liu, J. T. Surface Plasmon Resonance (SPR) combined technology: a powerful tool for investigating interface phenomena. *Adv. Mater. Interf.* **10**, https://doi.org/10.1002/admi.202202202 (2023).
11. Nicoletti, O. et al. Three-dimensional imaging of localized surface plasmon resonances of metal nanoparticles. *Nature* **502**, 80–84 (2013).
12. Sharar, N. et al. The employment of the surface plasmon resonance (SPR) microscopy sensor for the detection of individual extracellular vesicles and non-biological nanoparticles. *Biosensors* **13**, https://doi.org/10.3390/bios13040472 (2023).
13. Wong, P. C. et al. Plasma-enabled graphene quantum dot hydrogel-magnesium composites as bioactive scaffolds for in vivo bone defect repair. *ACS Appl. Mater. interfaces* **15**, 44607–44620 (2023).
14. Singh, P. SPR biosensors: historical perspectives and current challenges. *Sens. Actuators B Chem.* **229**, 110–130 (2016).
15. Zhou, J. et al. Surface plasmon resonance (SPR) biosensors for food allergen detection in food matrices. *Biosens. Bioelectron.* **142**, 111449 (2019).
16. Masson, J. F. Surface plasmon resonance clinical biosensors for medical diagnostics. *ACS Sens.* **2**, 16–30 (2017).
17. Zhang, X. et al. Excitation-detection integrated trapezoidal prism-coupled surface plasmon resonance based on a compact optical system. *Sens. Actuators B Chem.* **427**, 137234 (2025).
18. Maurya, P. & Verma, R. MIP integrated surface plasmon resonance in vitro detection of sodium benzoate. *Analyst* **148**, 1141–1150 (2023).
19. Liu, X. et al. In-situ profiling of glycosylation on single cells with surface plasmon resonance imaging. *Nat. Commun.* **16**, 1000 (2025).
20. Hong, M., Dawkins, R. B., Bertoni, B., You, C. & Magaña-Loaiza, O. S. Non-classical near-field dynamics of surface plasmons. *Nat. Phys.* **20**, 830–835 (2024).
21. Dienstbier, P. et al. Tracing attosecond electron emission from a nanometric metal tip. *Nature* **616**, 702–706 (2023).
22. Bolognesi, M. et al. A fully integrated miniaturized optical biosensor for fast and multiplexing plasmonic detection of high- and low-molecular-weight analytes. *Adv. Mater.* **35**, e2208719 (2023).
23. Liu, Z. et al. Ultrasensitive imaging-based sensor unlocked by differential guided-mode resonance. *Nat. Commun.* **16**, 6113 (2025).
24. Levy, D. & Camley, R. E. Enhancement of sensitivity in surface plasmon resonance. *AIP Adv.* **15**, https://doi.org/10.1063/5.0245116 (2025).
25. Yang, D. et al. Probing single-cell adhesion kinetics and nanomechanical force with surface plasmon resonance imaging. *ACS Nano* **19**, 2651–2664 (2025).
26. Naik, G. V., Shalaev, V. M. & Boltasseva, A. Alternative plasmonic materials: beyond gold and silver. *Adv. Mater.* **25**, 3264–3294 (2013).
27. Yuan, Y. et al. Highly anisotropic black phosphorous-graphene hybrid architecture for ultrassensitive plasmonic biosensing: theoretical insight. *2D Mater.* **5**, 025015 (2018).
28. Ouyang, Q. et al. Two-dimensional transition metal dichalcogenide enhanced phase-sensitive plasmonic biosensors: theoretical insight. *J. Phys. Chem. C.* **121**, 6282–6289 (2017).
29. Zeng, S. et al. Graphene-gold metasurface architectures for ultrasensitive plasmonic biosensing. *Adv. Mater.* **27**, 6163–6169 (2015).
30. Lei, Z. L. & Guo, B. 2D material-based optical biosensor: status and prospect. *Adv. Sci.* **9**, e2102924 (2022).
31. Philip, A. & Kumar, A. R. The performance enhancement of surface plasmon resonance optical sensors using nanomaterials: a review. *Coord. Chem. Rev.* **458**, 214424 (2022).
32. Wulandari, C., Septiani, N. L. W., Nugraha, N., Nuruddin, A. & Yuliarto, B. 2-dimensional materials for performance enhancement of surface plasmon resonance biosensor: review paper. *J. Eng. Technol. Sci.* **55**, 479–513 (2023).
33. Huo, Z. et al. Dual-mode colorimetric-SPR immunosensor based on gold nanoparticles for sCD146 detection in plasma. *Biosens. Bioelectron.* **287**, 117702 (2025).
34. Ansari, G., Pal, A., Srivastava, A. K. & Verma, G. Detection of hemoglobin concentration in human blood samples using a zinc oxide nanowire and graphene layer heterostructure based refractive index biosensor. *Opt. Laser Technol.* **164**, 109495 (2023).
35. Khodaie, A. & Heidarzadeh, H. Ultra-sensitive surface plasmon resonance sensor integrating MXene (Ti(3)C(2)T(X)) and graphene for advanced carcinoembryonic antigen detection. *Sci. Rep.* **15**, 13571 (2025).
36. Zhao, X. et al. Plasmonic trimers designed as SERS-active chemical traps for subtyping of lung tumors. *Nat. Commun.* **15**, 5855 (2024).
37. Halas, N. J., Lal, S., Chang, W. S., Link, S. & Nordlander, P. Plasmons in strongly coupled metallic nanostructures. *Chem. Rev.* **111**, 3913–3961 (2011).
38. Phan, Q. H. et al. Decomposition Mueller matrix polarimetry for enhanced miRNA detection with antimonene-based surface plasmon resonance

sensor and DNA-linked gold nanoparticle signal amplification. *Talanta* **270**, 125611 (2024).
39. Zayats, A. V., Smolyaninov, I. I. & Maradudin, A. A. Nano-optics of surface plasmon polaritons. *Phys. Rep.* **408**, 131–314 (2005).
40. Chen, R. et al. Highly sensitive surface plasmon resonance sensor with surface modified MoSe(2)/ZnO composite film for non-enzymatic glucose detection. *Biosens. Bioelectron.* **237**, 115469 (2023).
41. Wulandari, C. et al. Surface plasmon resonance biosensor chips integrated with MoS(2)-MoO(3) hybrid microflowers for rapid CFP-10 tuberculosis detection. *J. Mater. Chem. B* **11**, 11588–11599 (2023).
42. Liu, Y. et al. Cell membrane biomimetic nanoparticle-enhanced SPR biosensor for facile and sensitive detection of circulating tumor cells. *Sens. Actuators B Chem.* **440**, 137872 (2025).
43. Khomyakov, P. A. et al. First-principles study of the interaction and charge transfer between graphene and metals. *Phys. Rev. B* **79**, https://doi.org/10.1103/PhysRevB.79.195425 (2009).
44. Wang, Q. H., Kalantar-Zadeh, K., Kis, A., Coleman, J. N. & Strano, M. S. Electronics and optoelectronics of two-dimensional transition metal dichalcogenides. *Nat. Nanotechnol.* **7**, 699–712 (2012).
45. Yuan, Y. et al. Two-dimensional nanomaterials as enhanced surface plasmon resonance sensing platforms: design perspectives and illustrative applications. *Biosens. Bioelectron.* **241**, 115672 (2023).
46. Phan, Q.-H. et al. Antimonene-based surface plasmon resonance with antibody S9.6 signal amplification for miRNA detection. *Opt. Laser Technol.* **171**, 110452 (2024).
47. Banerjee, A., Rahul, R., Thangaraj, J. & Kumar, S. High-sensitivity SPR fiber-optic biosensor with nano-grating structure for pathogenic bacteria detection in drinking water. *IEEE Sens. J.* **24**, 36882–36890 (2024).
48. Kumar, A., Kumar, A., Srivastava, M., Prakash, R. & Srivastava, S. K. A graphene oxide assisted surface plasmon resonance sensor for chloroquine phosphate detection: a theoretical and experimental study. *Opt. Laser Technol.* **191**, 113341 (2025).
49. Hsieh, P. Y. et al. Integrated metasurfaces on silicon photonics for emission shaping and holographic projection. *Nanophotonics* **11**, 4687–4695 (2022).
50. Kuznetsov, A. I. et al. Roadmap for optical metasurfaces. *ACS Photonics* **11**, 816–865 (2024).
51. Fang, Z. & Zhu, X. Plasmonics in nanostructures. *Adv. Mater.* **25**, 3840–3856 (2013).
52. Lv, E. et al. Detection of multiple biometabolite molecules by SPR-SERS dual-functional biosensors based on highly sensitive ridge Hyperbolic Metamaterials. *Appl. Surf. Sci.* **702**, 163338 (2025).
53. Sang, W. et al. Wavelength sequential selection technique for high-throughput multi-channel phase interrogation surface plasmon resonance imaging sensing. *Talanta* **258**, 124405 (2023).
54. Hu, S. et al. Universal and flexible design for high-sensitivity and wide-ranging surface plasmon resonance sensors based on a three-dimensional tuning hypersurface. *Sens. Actuat. B Chem.* **380**, 133284 (2023).
55. Shokova, M. A. & Bochenkov, V. E. Impact of optical cavity on refractive index sensitivity of gold nanohole arrays. *Biosensors* **13**, https://doi.org/10.3390/bios13121038 (2023).
56. Uniyal, A., Pal, A., Ansari, G. & Chauhan, B. Numerical simulation of InP and MXene-based SPR sensor for different cancerous cells detection. *Cell Biochem. Biophys.* https://doi.org/10.1007/s12013-025-01675-9 (2025).
57. Yu, X. et al. Widening of dynamic detection range in real-time angular-interrogation surface plasmon resonance biosensor based on anisotropic van der Waals heterojunction. *Biosensors* **14**, https://doi.org/10.3390/bios14120601 (2024).
58. Rafi, S. A. et al. Optical based surface plasmon resonance sensor for the detection of the various kind of cancerous cell. *Cell Biochem. Biophys.* **83**, 689–715 (2025).
59. Singh, N. et al. Electrochemical and plasmonic detection of myocardial infarction using microfluidic biochip incorporated with mesoporous nanoscaffolds. *ACS Appl. Mater. Interfaces* **16**, 32794–32811 (2024).
60. Nuguri, S. M. et al. Stretchable metamaterials with Tamm/Fano resonances for tunable, efficient mechanochromic color shifting. *Adv. Opt. Mater.* **12**, https://doi.org/10.1002/adom.202400921 (2024).
61. Liu, H. et al. Advancing MicroRNA detection: enhanced biotin-streptavidin dual-mode phase imaging surface plasmon resonance aptasensor. *Anal. Chem.* **96**, 8791–8799 (2024).
62. Zeng, S. et al. Graphene–MoS2 hybrid nanostructures enhanced surface plasmon resonance biosensors. *Sens. Actuators B Chem.* **207**, 801–810 (2015).
63. Zhu, S. et al. Label-free biosensing with singular-phase-enhanced lateral position shift based on atomically thin plasmonic nanomaterials. *Light Sci. Appl.* **13**, 2 (2024).
64. Hashim, H. S. et al. Surface plasmon resonance sensor based on gold-graphene quantum dots thin film as a sensing nanomatrix for phenol detection. *Opt. Laser Technol.* **168**, 109816 (2024).
65. Chen, C. Y. et al. Clinical application of a graphene oxide-based surface plasmon resonance biosensor to measure first-trimester serum pregnancy-associated plasma protein-A/A2 ratio to predict preeclampsia. *Int. J. Nanomed.* **18**, 7469–7481 (2023).
66. Ouyang, J. et al. The synergistic effect of electric-field and adsorption enhancement of amino acid carbon dots significantly improves the detection sensitivity of SPR sensors. *Sensors* **25**, 3903 (2025).
67. Jain, P. K., Huang, X., El-Sayed, I. H. & El-Sayed, M. A. Review of some interesting surface plasmon resonance-enhanced properties of noble metal nanoparticles and their applications to biosystems. *Plasmonics* **2**, 107–118 (2007).
68. Khlebtsov, N. G. & Dykman, L. A. Optical properties and biomedical applications of plasmonic nanoparticles. *J. Quant. Spectrosc. Radiat. Transf.* **111**, 1–35 (2010).
69. Maier, S. A. Plasmonics: fundamentals and applications. *Springer Science +BusinessMedia LLC* **5**, 65–88 (2007).
70. Kawa, S. Near-field optics and surface plasmon polaritons: chapter: spectroscopy of gap modes in metal particle-surface systems. *Springer-Verlag Berlin Heidelberg New York* (2001).
71. Ruppin, R. Surface modes and optical absorption of a small sphere above a substrate. *Surf. Sci.* **127**, 108–118 (1983).
72. Wang, X. et al. A facile strategy to prepare dendrimer-stabilized gold nanorods with sub-10-nm size for efficient photothermal cancer therapy. *Sci. Rep.* **6**, 22764 (2016).
73. Sundaramurthy, A. et al. Field enhancement and gap-dependent resonance in a system of two opposing tip-to-tip Au nanotriangles. *Phys. Rev. B* **72**, https://doi.org/10.1103/PhysRevB.72.165409 (2005).
74. Gao, J. et al. A reliable gold nanoparticle/Cu-TCPP 2D MOF/gold/D-shaped fiber sensor based on SPR and LSPR coupling for dopamine detection. *Appl. Surf. Sci.* **655**, 159523 (2024).
75. Dillen, A. et al. Integrated signal amplification on a fiber optic SPR sensor using duplexed aptamers. *ACS Sens.* **8**, 811–821 (2023).
76. Deb, T., Pukhrambam, P. D., Panda, A. & Singh, G. Modeling of surface plasmon resonance (SPR) gas sensor using phase change material and black phosphorus for non-invasive diagnosis of lung and liver diseases. *Opt. Laser Technol.* **188**, 112959 (2025).
77. Nordlander, P. Plasmon hybridization in nanoparticles near metallic surfaces. *Nano Lett.* **4**, 2209–2213 (2004).
78. Yu, X. et al. Strong coupling in microcavity structures: principle, design, and practical application. *Laser Photon. Rev.* **13**, https://doi.org/10.1002/lpor.201800219 (2018).
79. Inou, I., Fujimoto, M. & Bando, K. Anticrossing behavior in nanolayered heterostructures caused by coupling between a planar waveguide mode in an anthracene single crystal and a silver surface plasmon polariton mode: implications for attenuated total reflection spectroscopy. *ACS Appl. Nano Mater.* **4**, 250–259 (2021).
80. Bansal, A. & Srivastava, S. K. High performance SPR sensor using 2-D materials: a treatise on design aspects, material choice and figure of merit. *Sens. Actuat. A Phys.* **369**, 115159 (2024).
81. Mohajer, S., Sharif, M. A., Aghdam, A. H., Borjkhani, M. & Assadi, M. H. N. Amplified hybrid surface plasmon polaritons in partially reduced graphene oxide supported on gold. *Appl. Surf. Sci.* **639**, 158120 (2023).
82. Pirker, L., Honolka, J., Velický, M. & Frank, O. When 2D materials meet metals. *2D Mater.* **11**, 022003 (2024).
83. Wu, L. et al. Sensitivity enhancement by using few-layer black phosphorus-graphene/TMDCs heterostructure in surface plasmon resonance biochemical sensor. *Sens. Actuat. B Chem.* **249**, 542–548 (2017).
84. Tan, J. et al. Two-dimensional material-enhanced surface plasmon resonance for antibiotic sensing. *J. Hazard. Mater.* **455**, 131644 (2023).
85. Wang, Y. et al. 2D MOF-enhanced SPR sensing platform: facile and ultra-sensitive detection of Sulfamethazine via supramolecular probe. *J. Hazard. Mater.* **456**, 131642 (2023).
86. Wang, Y. et al. Targeted sub-attomole cancer biomarker detection based on phase singularity 2D nanomaterial-enhanced plasmonic biosensor. *Nano-Micro Lett.* **13**, 96 (2021).

87. Cai, Y., Zhang, G. & Zhang, Y. W. Layer-dependent band alignment and work function of few-layer phosphorene. *Sci. Rep.* **4**, 6677 (2014).
88. Giovannetti, G. et al. Doping graphene with metal contacts. *Phys. Rev. Lett.* **101**, 026803 (2008).
89. Dykstra, G., Chapa, I. & Liu, Y. Reagent-free lactate detection using Prussian blue and electropolymerized-molecularly imprinted polymers-based electrochemical biosensors. *ACS Appl. Mater. interfaces* **16**, 66921–66931 (2024).
90. Feng, J. et al. Cu-Based Tris(chloropropyl) phosphate MOF nanosheets for surface plasmon resonance-based fiber-optic biosensing. *ACS Appl. Nano Mater.* **6**, 12775–12783 (2023).
91. Khomyakov, P. A. et al. First-principles study of the interaction and charge transfer between graphene and metals. *Phys. Rev. B* **79**, 195425 (2009).
92. Govorov, A. O. et al. Exciton-plasmon interaction and hybrid excitons in semiconductor-metal nanoparticle assemblies. *Nano Lett.* **6**, 984–994 (2006).
93. Cao, E., Lin, W., Sun, M., Liang, W. & Song, Y. Exciton-plasmon coupling interactions: from principle to applications. *Nanophotonics* **7**, 145–167 (2017).
94. Todisco, F., D'Agostino, S., Esposito, M., Fernàndez-Domìnguez, A. I. & Sanvitto, D. Exciton-plasmon coupling enhancement via metal oxidation. *ACS Nano* **9**, 9691–9699 (2015).
95. Cai, C., Bi, G. & Xu, T. Fano resonance in the CsPbBr 3 nanocrystal/Ag nanostructure through the exciton-plasmon coupling. *Appl. Phys. Lett.* **115**, 161602 (2019).
96. Yu, X., Wang, X., Zhou, F., Qu, J. & Song, J. 2D van der Waals heterojunction nanophotonic devices: from fabrication to performance. *Adv. Funct. Mater.* **31**, https://doi.org/10.1002/adfm.202104260 (2021).
97. Geim, A. K. & Grigorieva, I. V. Van der Waals heterostructures. *Nature* **499**, 419–425 (2013).
98. Zhang, X., Peng, H., Liu, J. & Yuan, Y. Highly sensitive plasmonic biosensor enhanced by perovskite-graphene hybrid configuration. *J. Opt.* **25**, 075002 (2023).
99. Du, F., Zheng, K., Zeng, S. & Yuan, Y. Sensitivity enhanced tunable plasmonic biosensor using two-dimensional twisted bilayer graphene superlattice. *Nanophotonics* **12**, 1271–1284 (2023).
100. Ee, H. S. & Agarwal, R. Tunable metasurface and flat optical zoom lens on a stretchable substrate. *Nano Lett.* **16**, 2818–2823 (2016).
101. Luo, Y. et al. Strong light-matter coupling in van der Waals materials. *Light Sci. Appl.* **13**, 203 (2024).
102. Lee, Y. M., Kim, S. E. & Park, J. E. Strong coupling in plasmonic metal nanoparticles. *Nano Convergence* **10**, 34 (2023).
103. Zhang, L. et al. Room-temperature exciton polaritons in a monolayer molecular crystal. *Nano Lett.* **24**, 16072–16080 (2024).
104. Niu, Y., Gao, L., Xu, H. & Wei, H. Strong coupling of multiple plasmon modes and excitons with excitation light controlled active tuning. *Nanophotonics* **12**, 735–742 (2023).
105. ElKabbash, M. et al. Fano resonant optical coatings platform for full gamut and high purity structural colors. *Nat. Commun.* **14**, 3960 (2023).
106. Wang, Z., Ho, Y. L., Cao, T., Yatsui, T. & Delaunay, J. J. High-Q and tailorable Fano resonances in a one-dimensional metal-optical Tamm state structure: from a narrowband perfect absorber to a narrowband perfect reflector. *Adv. Funct. Mater.* **31**, https://doi.org/10.1002/adfm.202102183 (2021).
107. Vabishchevich, P. P. et al. Enhanced second-harmonic generation using broken symmetry III–V semiconductor fano metasurfaces. *ACS Photonics* **5**, 1685–1690 (2018).
108. Lovera, A., Gallinet, B., Nordlander, P. & Martin, O. J. F. Mechanisms of fano resonances in coupled plasmonic systems. *ACS Nano* **7**, 9 (2013).
109. Halas, N. J. et al. A plethora of plasmonics from the laboratory for nanophotonics at Rice University. *Adv. Mater.* **24**, 4842–4877 (2012).
110. Yan, X. et al. Topologically reconfigurable room-temperature polariton condensates from bound states in the continuum in organic metasurfaces. *Nat. Commun.* **16**, 2375(1–8) (2025).
111. Marinica, D. C., Borisov, A. G. & Shabanov, S. V. Bound states in the continuum in photonics. *Phys. Rev. Lett.* **100**, 183902 (2008).
112. Rozman, N., Fan, K. & Padilla, W. J. Symmetry-broken high-Q terahertz quasi-bound states in the continuum. *ACS Photonics* **11**, 8 (2024).
113. Yu, X. et al. Spin Hall effect of light based on a surface plasmonic platform. *Nanophotonics* **10**, 3031–3048 (2021).
114. Wan, H. et al. Surface plasmon resonance biosensor chips: Fabrications and pharmaceutical applications. *J. Pharm. Biomed. Anal.* **265**, 117018 (2025).
115. Ran, C. et al. Recent development of gold nanochips in biosensing and biodiagnosis sensibilization strategies in vitro based on SPR, SERS and FRET optical properties. *Talanta* **282**, 126936 (2025).
116. Jiang, R., Li, B., Fang, C. & Wang, J. Metal/semiconductor hybrid nanostructures for plasmon-enhanced applications. *Adv. Mater.* **26**, 5274–5309 (2014).
117. Sardar, R., Funston, A. M., Mulvaney, P. & Murray, R. W. Gold nanoparticles: past, present, and future. *Langmuir* **25**, 13840–13851 (2009).
118. Romo-Herrera, J. M., Alvarez-Puebla, R. A. & Liz-Marzan, L. M. Controlled assembly of plasmonic colloidal nanoparticle clusters. *Nanoscale* **3**, 1304–1315 (2011).
119. Liu, H., Fu, Y., Yang, R., Guo, J. & Guo, J. Surface plasmonic biosensors: principles, designs and applications. *Analyst* **148**, 6146–6160 (2023).
120. Lv, Z., He, S., Wang, Y. & Zhu, X. Noble metal nanomaterials for NIR-triggered photothermal therapy in cancer. *Adv. Healthc. Mater.* **10**, e2001806 (2021).
121. Fotooh Abadi, L., Kumar, P., Paknikar, K., Gajbhiye, V. & Kulkarni, S. Tenofovir-tethered gold nanoparticles as a novel multifunctional long-acting anti-HIV therapy to overcome deficient drug delivery-: an in vivo proof of concept. *J. Nanobiotechnol.* **21**, 19 (2023).
122. Krage, C. et al. Three-dimensional polyglycerol-PEG-Based Hydrogels As A Universal High-sensitivity Platform for SPR Analysis. *Anal. Chem.* **97**, 6329–6337 (2025).
123. Tao, A. R., Habas, S. & Yang, P. Shape control of colloidal metal nanocrystals. *Small* **4**, 310–325 (2008).
124. Elahi, N., Kamali, M. & Baghersad, M. H. Recent biomedical applications of gold nanoparticles: a review. *Talanta* **184**, 537–556 (2018).
125. Zhang, L., Mazouzi, Y., Salmain, M., Liedberg, B. & Boujday, S. Antibody-Gold Nanoparticle Bioconjugates For Biosensors: Synthesis, Characterization And Selected Applications. *Biosens. Bioelectron.* **165**, 112370 (2020).
126. Rajendran, R. et al. Dimensionally integrated nanoarchitectonics for a novel composite from 0D, 1D, and 2D nanomaterials: RGO/CNT/CeO2 ternary nanocomposites with electrochemical performance. *J. Mater Chem. A* **2**, 18480–18487 (2014).
127. Alivisatos, A. P. Semiconductor clusters, nanocrystals, and quantum dots. *Science* **271**, 933–937 (1996).
128. Zhao, Y. S., Fu, H., Hu, F., Peng, A. D. & Yao, J. Multicolor emission from ordered assemblies of organic 1D nanomaterials. *Adv. Mater.* **19**, 3554–3558 (2007).
129. Zhang, X. et al. Protein interface redesign facilitates the transformation of nanocage building blocks to 1D and 2D nanomaterials. *Nat. Commun.* **12**, 4849(1-11) (2021).
130. Panigrahi, S. et al. Synthesis and size-selective catalysis by supported gold nanoparticles: study on heterogeneous and homogeneous catalytic process. *J. Phys. Chem. C* **111**, 4596–4605 (2007).
131. Spear, N. J. et al. Surface plasmon mediated harmonically resonant effects on third harmonic generation from Au and CuS nanoparticle films. *Nanophotonics* **12**, 273–284 (2023).
132. Yin, P. T., Shah, S., Chhowalla, M. & Lee, K. B. Design, synthesis, and characterization of graphene-nanoparticle hybrid materials for bioapplications. *Chem. Rev.* **115**, 2483–2531 (2015).
133. Giljohann, D. A. et al. Gold nanoparticles for biology and medicine. *Angew. Chem.* **49**, 3280–3294 (2010).
134. Zhang, L., Niu, W. & Xu, G. Synthesis and applications of noble metal nanocrystals with high-energy facets. *Nano Today* **7**, 586–605 (2012).
135. Xiao, J. & Qi, L. Surfactant-assisted, shape-controlled synthesis of gold nanocrystals. *Nanoscale* **3**, 1383–1396 (2011).
136. Xia, Y., Xia, X., Wang, Y. & Xie, S. Shape-controlled synthesis of metal nanocrystals. *MRS Bull.* **38**, 335–344 (2013).
137. Ojea-Jime´nez, I. & Puntes, V. Instability of cationic gold nanoparticle bioconjugates: the role of citrate ions. *J. Am. Chem. Soc.* **131**, 7 (2009).
138. Daruich De Souza, C., Ribeiro Nogueira, B. & Rostelato, M. E. C. M. Review of the methodologies used in the synthesis gold nanoparticles by chemical reduction. *J. Alloy. Compd.* **798**, 714–740 (2019).
139. Loza, K., Heggen, M. & Epple, M. Synthesis, structure, properties, and applications of bimetallic nanoparticles of noble metals. *Adv. Funct. Mater.* **30**, https://doi.org/10.1002/adfm.201909260 (2020).
140. Grzelczak, M., Perez-Juste, J., Mulvaney, P. & Liz-Marzan, L. M. Shape control in gold nanoparticle synthesis. *Chem. Soc. Rev.* **37**, 1783–1791 (2008).

141. Fievet, F. et al. The polyol process: a unique method for easy access to metal nanoparticles with tailored sizes, shapes and compositions. *Chem. Soc. Rev.* **47**, 5187–5233 (2018).
142. Kang, H. et al. Stabilization of silver and gold nanoparticles: preservation and improvement of plasmonic functionalities. *Chem. Rev.* **119**, 664–699 (2019).
143. Krishnamurthy, S. & Yun, Y.-S. Recovery of microbially synthesized gold nanoparticles using sodium citrate and detergents. *Chem. Eng. J.* **214**, 253–261 (2013).
144. Wang, Y., He, J., Liu, C., Chong, W. H. & Chen, H. Thermodynamics versus kinetics in nanosynthesis. *Angew. Chem.* **54**, 2022–2051 (2015).
145. Heuer-Jungemann, A. et al. The role of ligands in the chemical synthesis and applications of inorganic nanoparticles. *Chem. Rev.* **119**, 4819–4880 (2019).
146. Carbone, L. & Cozzoli, P. D. Colloidal heterostructured nanocrystals: Synthesis and growth mechanisms. *Nano Today* **5**, 449–493 (2010).
147. MariaWuithschick, A. B. et al. Turkevich in new robes: key questions answered for the most common gold nanoparticle synthesis. *ACS Nano* **9**, 7052–7071 (2015).
148. Lee, H. B., Yoo, Y. M. & Han, Y.-H. Characteristic optical properties and synthesis of gold–silica core–shell colloids. *Scr. Mater.* **55**, 1127–1129 (2006).
149. Zhang, G., Liu, Q., Xu, C. & Li, B. Uncovering origin of chirality of gold nanoparticles prepared through the conventional citrate reduction method. *Anal. Chem.* **95**, 6107–6114 (2023).
150. Sugawa, K. et al. Fabrication of dense two-dimensional assemblies over vast areas comprising gold(core)-silver(shell) nanoparticles and their surface-enhanced Raman scattering properties. *Photochem. Photobiol. Sci. Off. J. Eur. Photochem. Assoc. Eur. Soc. Photobiol.* **13**, 82–91 (2014).
151. Raposo, B. L. et al. A novel strategy based on Zn(II) porphyrins and silver nanoparticles to photoinactivate candida albicans. *Int. J. Nanomed.* **18**, 3007–3020 (2023).
152. Uechi, I. & Yamada, S. Photochemical and analytical applications of gold nanoparticles and nanorods utilizing surface plasmon resonance. *Anal. Bioanal. Chem.* **391**, 2411–2421 (2008).
153. Wu, T. et al. Self-driving lab for the photochemical synthesis of plasmonic nanoparticles with targeted structural and optical properties. *Nat. Commun.* **16**, 1473 (2025).
154. Gunawardana, N., Ke, C.-Y., Huang, C.-L. & Yang, C.-H. One-pot synthesis of near-infrared absorbing silver nanoprisms via a simple photochemical method using an ultraviolet-C light source. *Opt. Mater.* **148**, 114932 (2024).
155. Huang, W. L., Liao, W. H. & Chu, S. Y. Application of a perovskite NIR-LED with highly stable FAPbI(3)@SiO(2) core-shell nanocomposites in a SPR sensing platform. *ACS Appl. Mater. Interf.* **15**, 41151–41161 (2023).
156. Fan, G. et al. Mechanism for the photoreduction of poly(vinylpyrrolidone) to HAuCl4 and the dominating saturable absorption of Au colloids. *Phys. Chem. Chem. Phys.* **18**, 8993–9004 (2016).
157. Shafey, A. M. E. Green synthesis of metal and metal oxide nanoparticles from plant leaf extracts and their applications: a review. *Green. Process. Synth.* **9**, 304–339 (2020).
158. Duan, H., Wang, D. & Li, Y. Green chemistry for nanoparticle synthesis. *Chem. Soc. Rev.* **44**, 5778–5792 (2015).
159. Onitsuka, S., Hamada, T. & Okamura, H. Preparation of antimicrobial gold and silver nanoparticles from tea leaf extracts. *Colloids Surf. B Biointerfaces* **173**, 242–248 (2019).
160. Singh, N., Batra, U., Kumar, K., Ahuja, N. & Mahapatro, A. Progress in bioactive surface coatings on biodegradable Mg alloys: a critical review towards clinical translation. *Bioact. Mater.* **19**, 717–757 (2023).
161. Zheng, J. et al. Gold nanorods: the most versatile plasmonic nanoparticles. *Chem. Rev.* **121**, 13342–13453 (2021).
162. Jiang, L. et al. Free-standing one-dimensional plasmonic nanostructures. *Nanoscale* **4**, 66–75 (2012).
163. Chen, Y. S., Zhao, Y., Yoon, S. J., Gambhir, S. S. & Emelianov, S. Miniature gold nanorods for photoacoustic molecular imaging in the second near-infrared optical window. *Nat. Nanotechnol.* **14**, 465–472 (2019).
164. Bastus, N. G., Comenge, J. & Puntes, V. Kinetically controlled seeded growth synthesis of citrate-stabilized gold nanoparticles of up to 200 nm: size focusing versus Ostwald ripening. *Langmuir* **27**, 11098–11105 (2011).
165. Sau, T. K. & Murphy, C. J. Seeded high yield synthesis of short Au nanorods in aqueous solution. *Langmuir* **20**, 6414–6420 (2004).
166. Chen, H., Shao, L., Li, Q. & Wang, J. Gold nanorods and their plasmonic properties. *Chem. Soc. Rev.* **42**, 2679–2724 (2013).
167. Sanchez-Iglesias, A., Jenkinson, K., Bals, S. & Liz-Marzan, L. M. Kinetic regulation of the synthesis of pentatwinned gold nanorods below room temperature. *J. Phys. Chem. C Nanomater. Interfaces* **125**, 23937–23944 (2021).
168. Wu, G. et al. A general synthesis approach for amorphous noble metal nanosheets. *Nat. Commun.* **10**, 4855 (2019).
169. Zhan, Y., Liu, Z., Najmaei, S., Ajayan, P. M. & Lou, J. Large-area vapor-phase growth and characterization of MoS(2) atomic layers on a SiO(2) substrate. *Small* **8**, 966–971 (2012).
170. Liu, X. et al. Thin-film electronics based on all-2D van der Waals heterostructures. *J. Inf. Disp.* **22**, 231–245 (2021).
171. Gong, Y. et al. Vertical and in-plane heterostructures from WS2/MoS2 monolayers. *Nat. Mater.* **13**, 1135–1142 (2014).
172. Yao, Y. et al. Prospective of magnetron sputtering for interface design in rechargeable lithium batteries. *Adv. Energy Mater.* **14**, https://doi.org/10.1002/aenm.202403117 (2024).
173. Han, T., Liu, H., Wang, S., Chen, S. & Yang, K. Research on the preparation and spectral characteristics of graphene/TMDs hetero-structures. *Nanoscale Res. Lett.* **15**, 219 (2020).
174. Kang, M. et al. Asymmetric charge distribution boosts hydrogen evolution performance in two-dimensional MoO2/MoS2 step heterostructure. *Carbon Energy* **7**, https://doi.org/10.1002/cey2.663 (2025).
175. Narayan, R., Lim, J., Jeon, T., Li, D. J. & Kim, S. O. Perylene tetracarboxylate surfactant assisted liquid phase exfoliation of graphite into graphene nanosheets with facile re-dispersibility in aqueous/organic polar solvents. *Carbon* **119**, 555–568 (2017).
176. Wang, Y. et al. Ultrafast synthesis of MXenes in minutes via low-temperature molten salt etching. *Adv. Mater.* **36**, https://doi.org/10.1002/adma.202410736 (2024).
177. Peng, J. & Weng, J. One-pot solution-phase preparation of a MoS2/graphene oxide hybrid. *Carbon* **94**, 568–576 (2015).
178. Zheng, X. et al. Solution-processed Graphene-MoS2 heterostructure for efficient hole extraction in organic solar cells. *Carbon* **142**, 156–163 (2019).
179. Sin Tan, Y., Wang, H., Wang, H., Pan, C. & Yang, J. K. W. High-throughput fabrication of large-scale metasurfaces using electron-beam lithography with SU-8 gratings for multilevel security printing. *Photonics Res.* **11**, B103 (2023).
180. Xu, Z. et al. Groove-structured metasurfaces for modulation of surface plasmon propagation. *Appl. Phys. Express* **7**, 052001 (2014).
181. Choi, S., Zuo, J., Das, N., Yao, Y. & Wang, C. Scalable nanoimprint manufacturing of functional multilayer metasurface devices. *Adv. Funct. Mater.* **34**, https://doi.org/10.1002/adfm.202404852 (2024).
182. Zhang, H. et al. Colloidal self-assembly based all-metal metasurface absorbers to achieve broadband, polarization-independent light absorption at UV–Vis frequencies. *Appl. Surf. Sci.* **584**, 152624 (2022).
183. Jue, J. et al. Three-photon direct laser writing of the QD-polymer metasurface for large field-of-view optical holography. *ACS Appl. Mater. interfaces* **17**, 14520–14526 (2025).
184. Kim, J. Y. et al. Highly tunable refractive index visible-light metasurface from block copolymer self-assembly. *Nat. Commun.* **7**, 12911 (2016).
185. Mutalik, C., Sharma, S., Yougbare, S., Chen, C. Y. & Kuo, T. R. Nanoplasmonic biosensors: a comprehensive overview and future prospects. *Int. J. Nanomed.* **20**, 5817–5836 (2025).
186. Li, G. et al. Wearable hydrogel SERS chip utilizing plasmonic trimers for uric acid analysis in sweat. *Nano Lett.* **24**, 13447–13454 (2024).
187. Xie, J. et al. Advances in surface plasmon resonance for analyzing active components in traditional Chinese medicine. *J. Pharm. Anal.* **14**, 100983 (2024).
188. Uniyal, A., Srivastava, G., Pal, A., Taya, S. & Muduli, A. Recent advances in optical biosensors for sensing applications: a review. *Plasmonics* **18**, 735–750 (2023).
189. Islam, M. A. & Masson, J. F. Plasmonic biosensors for health monitoring: inflammation biomarker detection. *ACS Sens.* **10**, 577–601 (2025).
190. Das, S., Devireddy, R. & Gartia, M. R. Surface Plasmon Resonance (SPR) sensor for cancer biomarker detection. *Biosensors* **13**, https://doi.org/10.3390/bios13030396 (2023).
191. Das, C. M. et al. Computational modeling for intelligent surface plasmon resonance sensor design and experimental schemes for real-time plasmonic biosensing: a review. *Adv. Theory Simulat.* **6**, https://doi.org/10.1002/adts.202200886 (2023).
192. Nasiri, H., Abbasian, K. & Baghban, H. Sensing of lactose by graphitic carbon nitride/magnetic chitosan composites with surface plasmon resonance method. *Food Biosci.* **61**, 104718 (2024).

193. Chen, L. C. et al. Facile and unplugged surface plasmon resonance biosensor with NIR-emitting perovskite nanocomposites for fast detection of SARS-CoV-2. *Anal. Chem.* **95**, 7186–7194 (2023).
194. Tene, T. et al. SARS-CoV-2 detection by surface plasmon resonance biosensors based on graphene-multilayer structures. *Front. Phys.* **12**, https://doi.org/10.3389/fphy.2024.1503400 (2024).
195. Xu, Y. et al. Sensitivity-enhanced plasmonic sensor modified with ZIF-8. *Opt. Laser Technol.* **181**, 111885 (2025).
196. Yin, Z., Jing, X. & Li, S. Cascade amplification-based triple probe biosensor for high-precision DNA hybridization detection of lung cancer gene. *APL Photonics* **9**, https://doi.org/10.1063/5.0228760 (2024).
197. Lertvachirapaiboon, C. et al. Transmission surface plasmon resonance imaging of silver nanoprisms enhanced propagating surface plasmon resonance on a metallic grating structure. *Sens. Actuat. B Chem.* **249**, 39–43 (2017).
198. Zhang, J. et al. Azimuthal scanning excitation surface plasmon resonance holographic microscopy. *Laser Photon. Rev.* **18**, https://doi.org/10.1002/lpor.202301013 (2024).
199. Schuster, S. C., Swanson, R. V., Alex, L. A., Bourret, R. B. & Simon, M. I. Assembly and function of a quaternary signal transduction complex monitored by surface plasmon resonance. *Nature* **365**, 343–347 (1993).
200. Cao, Y., Yang, S., Wang, D., Wang, J. & Ye, Y. H. Surface plasmon-enhanced dark-field microsphere-assisted microscopy. *Opt. express* **31**, 8641–8649 (2023).
201. Hou, J. et al. Rapid and reliable ultrasensitive detection of pathogenic H9N2 viruses through virus-binding phage nanofibers decorated with gold nanoparticles. *Biosens. Bioelectron.* **237**, 115423 (2023).
202. You, X. et al. Large field-of-view plasmonic scattering imaging and sensing of nanoparticles with isotropic point-spread-function. *Nat. Commun.* **16**, https://doi.org/10.1038/s41467-025-60460-7 (2025).
203. Wang, Y., Zhong, S., Lee, J. & Chen, H. 2D/0D heterojunction interface with photovoltaic enhancement and stabilization for label-free exosome biosensor. *Adv. Funct. Mater.* **34**, https://doi.org/10.1002/adfm.202405272 (2024).
204. Lin, P. Y. et al. pH-responsive triplex DNA nanoswitches: surface plasmon resonance platform for bladder cancer-associated microRNAs. *ACS Nano* **19**, 7140–7153 (2025).
205. Zhou, Y. et al. MoS2-mediated gap-mode surface plasmon enhancement: construction of SPR biosensor for direct detection of LECT2. *Sens. Actuators B Chem.* **425**, 136938 (2025).
206. Tan, J. et al. Ultrasensitive screening of endocrine-disrupting chemicals using a surface plasmon resonance biosensor with polarization-compensated laser heterodyne feedback. *Anal. Chem.* **95**, 8687–8695 (2023).
207. Liu, H. et al. Construction of a sensitive SWCNTs integrated SPR biosensor for detecting PD-L1(+) exosomes based on Fe(3)O(4)@TiO(2) specific enrichment and signal amplification. *Biosens. Bioelectron.* **262**, 116527 (2024).
208. Mao, Z. et al. Multifunctional DNA scaffold mediated gap plasmon resonance: application to sensitive PD-L1 sensor. *Biosens. Bioelectron.* **247**, 115938 (2024).
209. Zhang, Y. et al. Ti(3)C(2) MXene/GNRs for synergistically highly enhanced sensitivity of optical fiber SPR acetylcholine biosensors via an electrostatic layer-by-layer assembly method. *Biosens. Bioelectron.* **273**, 117146 (2025).
210. Liu, X. et al. Ultrawideband solid-state terahertz phase shifter electrically modulated by tunable conductive interface in total internal reflection geometry. *ACS Photonics* **11**, 2595–2603 (2024).
211. Chen, S. -h, Lin, H. -b, Wang, X. -z, Hu, S. -q & Luo, Y. -h Enhanced sensitivity of a surface plasmon resonance biosensor utilizing Au/ITO hyperbolic metamaterial. *Results Phys.* **49**, 106522 (2023).
212. Bhatt, P., Kaur, K. & George, J. Enhanced charge transport in two-dimensional materials through light-matter strong coupling. *ACS Nano* **15**, 13616–13622 (2021).
213. Ghosh, S., Yang, C. J. & Lai, J. Y. Optically active two-dimensional MoS(2)-based nanohybrids for various biosensing applications: a comprehensive review. *Biosens. Bioelectron.* **246**, 115861 (2024).
214. Wang, Y. et al. Interface-engineered 2d heterojunction with photoelectric dual gain: Mxene@MOF-enhanced SPR spectroscopy for direct sensing of exosomes. *Small* **20**, e2308897 (2024).
215. Jia, Q. et al. Insight into the promotion mechanism of the surface plasmon resonance aptasensor based on ultrathin MBene nanosheets embedded with aptamer-templated silver nanoclusters for aptasensing exosomal marker. *Talanta* **288**, 127716 (2025).
216. Zhao, B. et al. Extreme sensitivity biosensing platform based on Fano resonance and graphene oxide. *Sens. Actuators B Chem.* **438**, 137788 (2025).
217. Bylinkin, A. et al. Dual-band coupling of phonon and surface plasmon polaritons with vibrational and electronic excitations in molecules. *Nano Lett.* **23**, 3985–3993 (2023).
218. Wang, Y. et al. Nanopore confinement effect mediated heterogeneous plasmonic metasurfaces for multifunctional biosensing interfaces. *Small* **21**, e2408705 (2025).
219. Chen, M. et al. Nanoplasmonic affinity analysis system for molecular screening based on bright-field imaging. *Adv. Funct. Mater.* **34**, https://doi.org/10.1002/adfm.202314481 (2024).
220. Zhou, Y. et al. Tunable Au@SiO(2)/Au film metasurface as surface plasmon resonance enhancer for direct and ultrasensitive detection of exosomes. *Anal. Chem.* **95**, 9663–9671 (2023).
221. Lee, J. et al. Plasmonic biosensor enabled by resonant quantum tunnelling. *Nat. Photonics* **19**, 938–945 (2025).
222. Ding, L. et al. Highly sensitive and selective detection of cortisol using a novel SPR-aptamer sensor modified by gold nanoparticles. *IEEE Sens. J.* **24**, 4199 (2024).